$$h_w = 1024 \left(\mu_L / \mu_{sL}\right)^{-0.34} U_g^{0.316} \qquad 6.52$$

where

$$\mu_{sL} = \mu_L (1 + 4.5 v_s) \qquad 6.53$$

In the limit when $\mu_{sL} = \mu_L$, Eq. (6.52) reduces to Eq. (6.51). Figure 6.11 presents a comparison of all the four sets of data with the computed values based on Eq. (6.52). The good agreement between the computed and experimental values is a good testimony of the fact that slurry rheology is an important feature in correlating heat transfer data for three-phase systems.

Nitrogen-Therminol system heat transfer data of Saxena et al. [121], Fig. 4.66, for the thirty-seven tube bundle are synthesized in Fig. 6.12 on the basis of an empirical equation of the type (6.51). The exponent b is seen to be dependent upon temperature and decreases monotonically with increase in temperature. This effectively implies that our present data are not adequately represented by the theory of Deckwer et al. [51, 93].

6.4. Comparison of Present Three-Phase Data with Theory

The experimental data of Saxena et al. [122] for the air-water-red iron oxide are reported in Figs. 4.26 and 4.27 for a single probe in the small column at ambient conditions. In Figs. 6.13, these data are shown compared with the predictions of four models. On the whole, agreement between theory and experiment is poor and inadequate.

It is clear from Fig. 6.13 that none of the models can represent even qualitatively the experimental variation of h_w with U_g. The experimental values clearly display a trend of decreasing rate with increasing U_g and may even approach a constant value as the value of U_g is further increased. On the other hand all the models suggest an initial rapid and then a relatively gradual increase in h_W values with increasing U_g values. This failure of theory to predict even the qualitative trend of h_w dependence on U_g for slurries involving

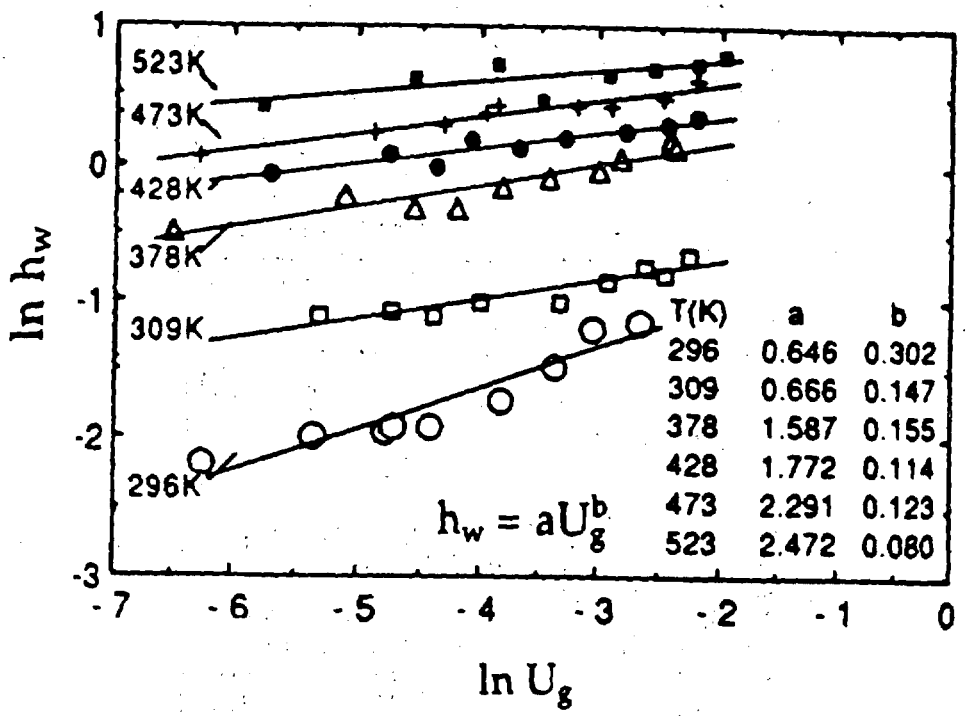

Fig. 6.12. A plot of heat transfer coefficient (probe 1) versus nitrogen velocity shown in logarithmic coordinates at different temperatures. Solids concentration = 0 wt%.

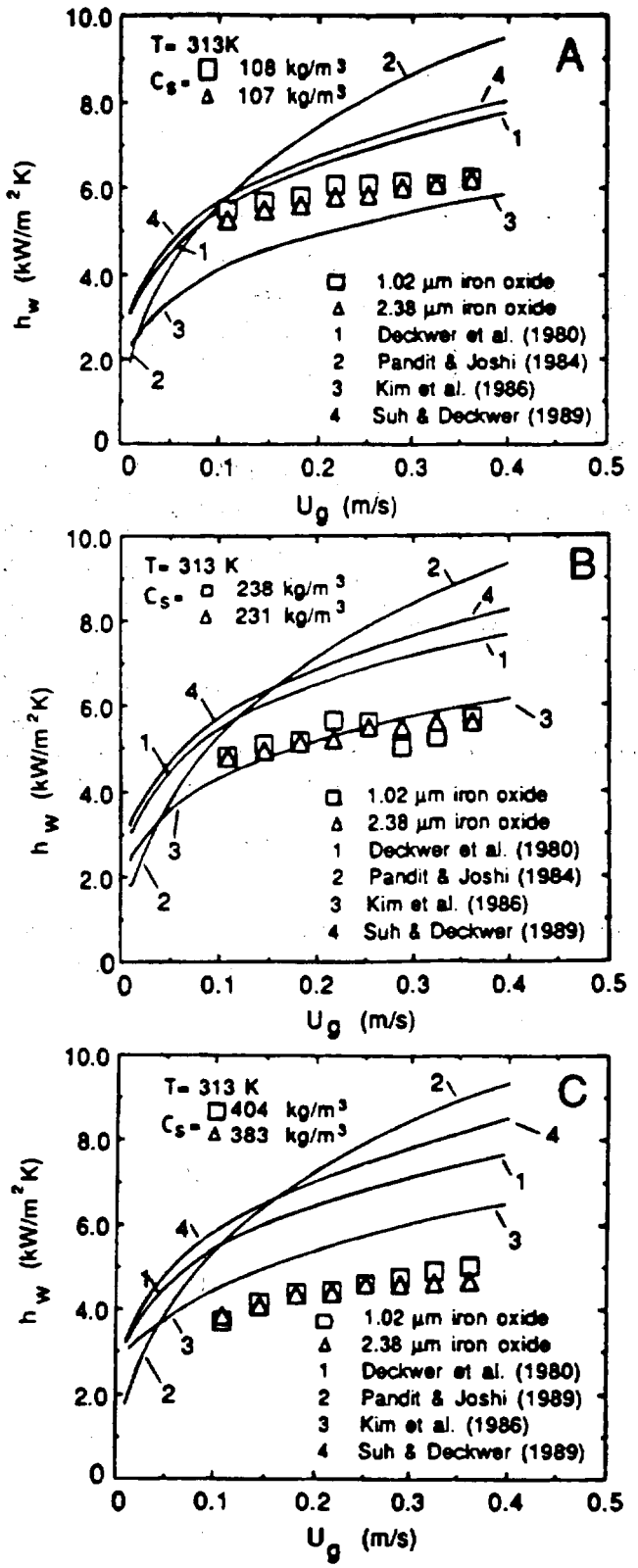

Fig. 6.13. Comparison of experimental h_W values as a function of U_g with the predictions of four theoretical models for slurries of two different average size particles at concentrations of (A) 107 and 108, (B) 231 and 238, and (C) 383 and 404 kg/m^3.

fine powders is a significant indicator for probing the differences in mechanistic details of heat transfer for slurries of small and large particles.

The quantitative predictions of these models are also in unsatisfactory agreement with the experimental values of heat transfer coefficient. The computed values based on Deckwer et al. theory (curves 1) are consistently and systematically greater than the corresponding experimental values. The degree of disagreement increases with increase in velocity beyond 0.1 m/s where the three-phase dispersion is in churn turbulent regime. Pandit and Joshi [106] correlation based values (curves 2) are always greater than Deckwer et al. [51] correlation based values for experimental values. However, their trend of reproduction of experimental data with respect to slurry concentration and gas velocity is disturbing. At the lowest slurry concentration, the computed values underestimate the experimental results over the entire air velocity range; at a still higher concentration in Fig. 6.13B the experimental data are somewhat satisfactorily reproduced; while at the highest slurry concentration in Fig. 6.13C, the calculated values (curves 3) overestimate the experimental data over the entire air velocity range.

Several empirical forms have been examined to represent the experimental data sets. The two successful empirical forms are those of Eq. (6.51) and

$$h_w = c + d \ln U_g \qquad 6.54$$

Heat transfer data for each slurry concentration and particle size were synthesized by the method of least-squares for the above mentioned two functional forms. The two constants a and b of Eq. (6.51) and c and d of Eq. (6.54) thus obtained are listed in Table 6.1 along with the range of air velocity. Also shown in this table are the values of average percentage absolute deviation and the range of percentage absolute deviation for h_w in each case. From the magnitudes of these deviations, it is clear that both of these functions are appropriate to represent the present data. The adequacy of these two functions to represent the heat transfer data is shown by the two parity plots of Figs. 6.14 and 6.15. In all cases, the heat transfer data are adequately represented by these t c functions within the limits of experimental uncertainty of $\pm$ 5 percent.

Table 6.1. Constants of Eqs. (6.51) and (6.54) as determined from the experimental h_W values for air-water-red iron oxide system at 313K and measured in 0.108 m bubble column equipped with 19 mm heat transfer probe.

System	d_p (μm)	C_s (kg/m^3)	Velocity range (m/s)	Constants		% Abs. Dev. Avg.	% Abs. Dev. Range
Equation 1:		$h_W = a\ U_g^b$		a	b		
Air - Water -	1.02	108	0.108 - 0.362	6.97	0.103	0.91	0.32 - 2.43
Iron oxide	1.02	238	0.108 - 0.362	6.09	0.093	3.74	0.09 - 8.50
(313 K)	1.02	404	0.108 - 0.362	6.34	0.228	1.11	0.19 - 2.38
	2.38	107	0.108 - 0.362	7.09	0.134	0.36	0.01 - 0.73
	2.38	231	0.108 - 0.362	6.52	0.139	0.80	0.17 - 2.06
	2.38	383	0.108 - 0.362	5.64	0.164	1.10	0.04 - 2.12
	All Data Based Global Constants			6.42	0.144	10.6	0.83 - 24.4
Equation 2:		$h_W = c + d \ln U_g$		c	d		
Air - Water -	1.02	108	0.108 - 0.362	6.88	0.610	0.88	0.22 - 2.35
Iron oxide	1.02	238	0.108 - 0.362	6.04	0.490	3.72	0.10 - 8.64
(313 K)	1.02	404	0.108 - 0.362	6.02	1.000	1.09	0.30 - 1.96
	2.38	107	0.108 - 0.362	6.95	0.770	0.39	0.02 - 0.83
	2.38	231	0.108 - 0.362	6.39	0.726	0.80	0.02 - 1.96
	2.38	383	0.108 - 0.362	5.48	0.706	0.97	0.00 - 2.00
	All Data Based Global Constants			6.29	0.716	10.5	0.01 - 25.3

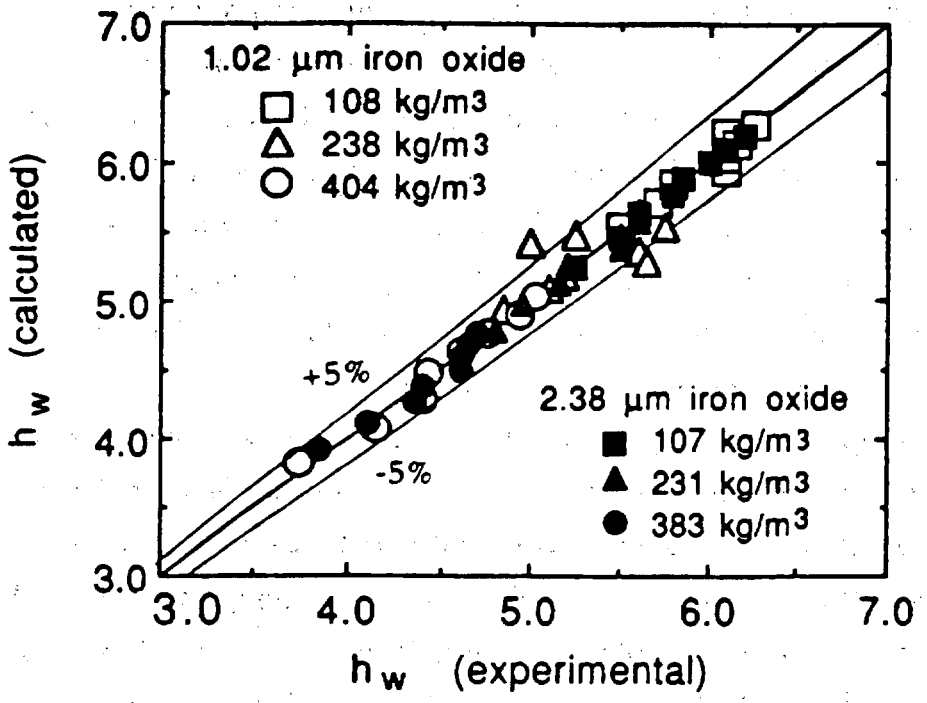

Fig. 6.14. Parity plot of h_W (kW/m^{2}K) for air-water-red iron oxide based on Eq. (6.51), power function, with the values of the constants listed in Table 6.1.

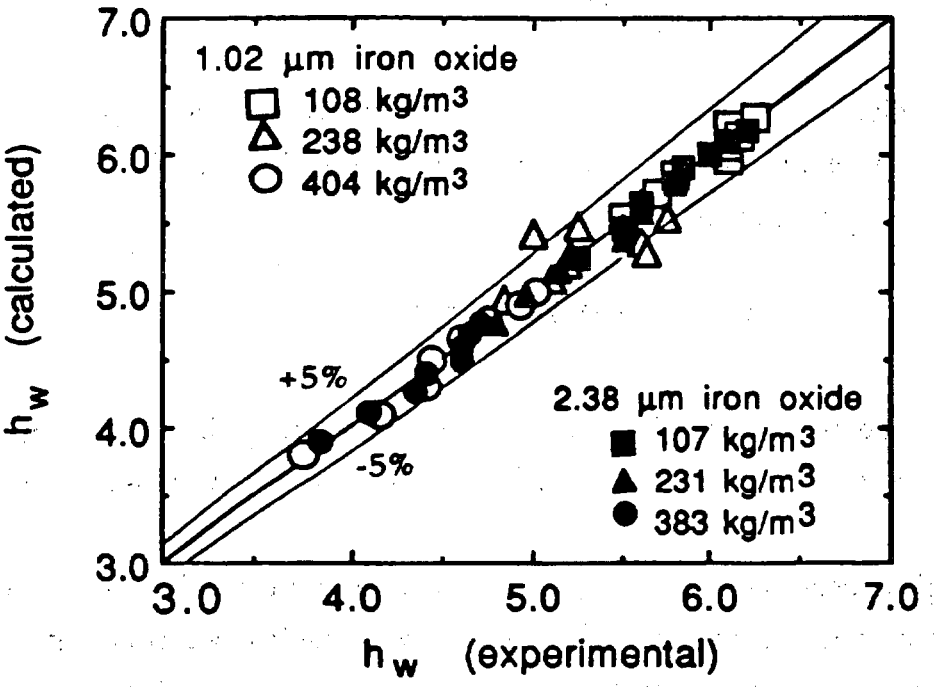

Fig. 6.15. Parity plot of h_W (kW/m^{2}K) for air-water-iron-oxide based on Eq. (6.54), logarithmic function, with the values of the constants listed in Table 6.1.

Next, an attempt was made to represent the entire data referring to two particle sizes, three concentrations for each particle size, and over the entire air velocity range by the two functions of Eqs. (6.51) and (6.54) but with only one set of constants for each function. This yielded the results graphed in Fig. 6.14A for the power function, and in Fig. 6.16B for the logarithmic function. The constants a and b, and c and d are listed in Table 6.1, and are referred to as global constants. It is clear that the reproduction is poor and unsatisfactory. The maximum deviation ranges up to as much as twenty-five percent.

To discover the reason for this large discrepancy we examined the role of suspension rheology in heat transfer process. Particles smaller than 10 μm but closer to 1 μm are generally considered colloidal and these remain more or less dispersed in suspension under gravity, Probstein and Sengun [123]. These authors have proposed that the rheology characteristics of a suspension is largely controlled by the volume fraction of the colloidal particles. Hence, it will be appropriate to introduce the suspension viscosity term in the above empirical expression to account for the changing heat transfer behavior as the slurry concentration is altered. Hence Eq. (6.51) is rewritten in the following form:

$$h_w = a' \mu_s^e U_g^b \qquad 6.55$$

Here, the suspension viscosity, μ_{SL}, is defined in terms of the liquid phase viscosity, μ_L, by the relation of Eq. (6.27). A regression analysis of the entire data leads to the following explicit relationship:

$$h_w = 8.13 (\mu_L/\mu_s)^{1.14} U_g^{0.144} \qquad 6.56$$

The adequacy of the proposed relationship of Eq. (6.56) is to be judged by the parity plot of Fig. 6.17 giving the calculated and experimental heat transfer coefficients.

Air-water-glass bead system data [69, 127], as obtained in the small column with a single probe and for slurries of different size particles and concentrations is compared with the predictions of different models in Fig. 6.18. Kim et al. [107] correlation based values (curve 3) are always smaller while those of Pandit and

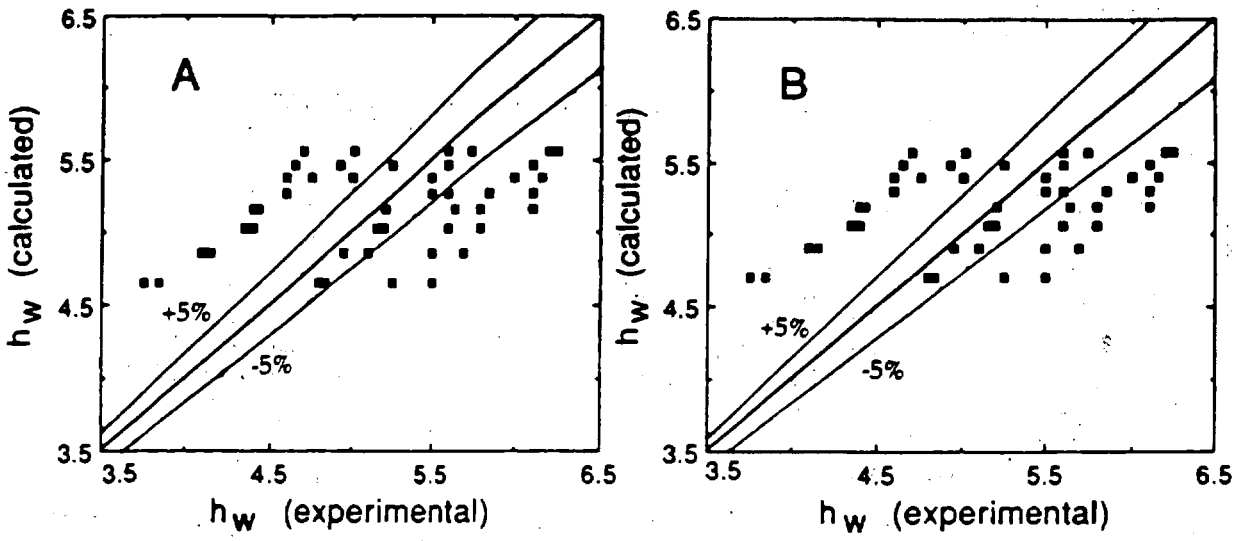

Fig. 6.16. Parity plot of h_W (kW/m^{2}K) for air-water-iron-oxide system with global constants: (A) power function, and (B) logarithmic function.

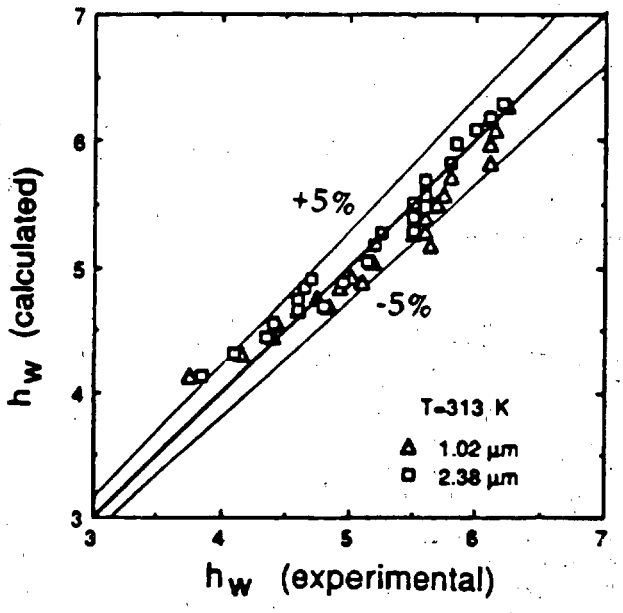

Fig. 6.17. Parity plot of h_W (kW/m^{2}K) for air-water-iron oxide system based on Eq. (6.56).

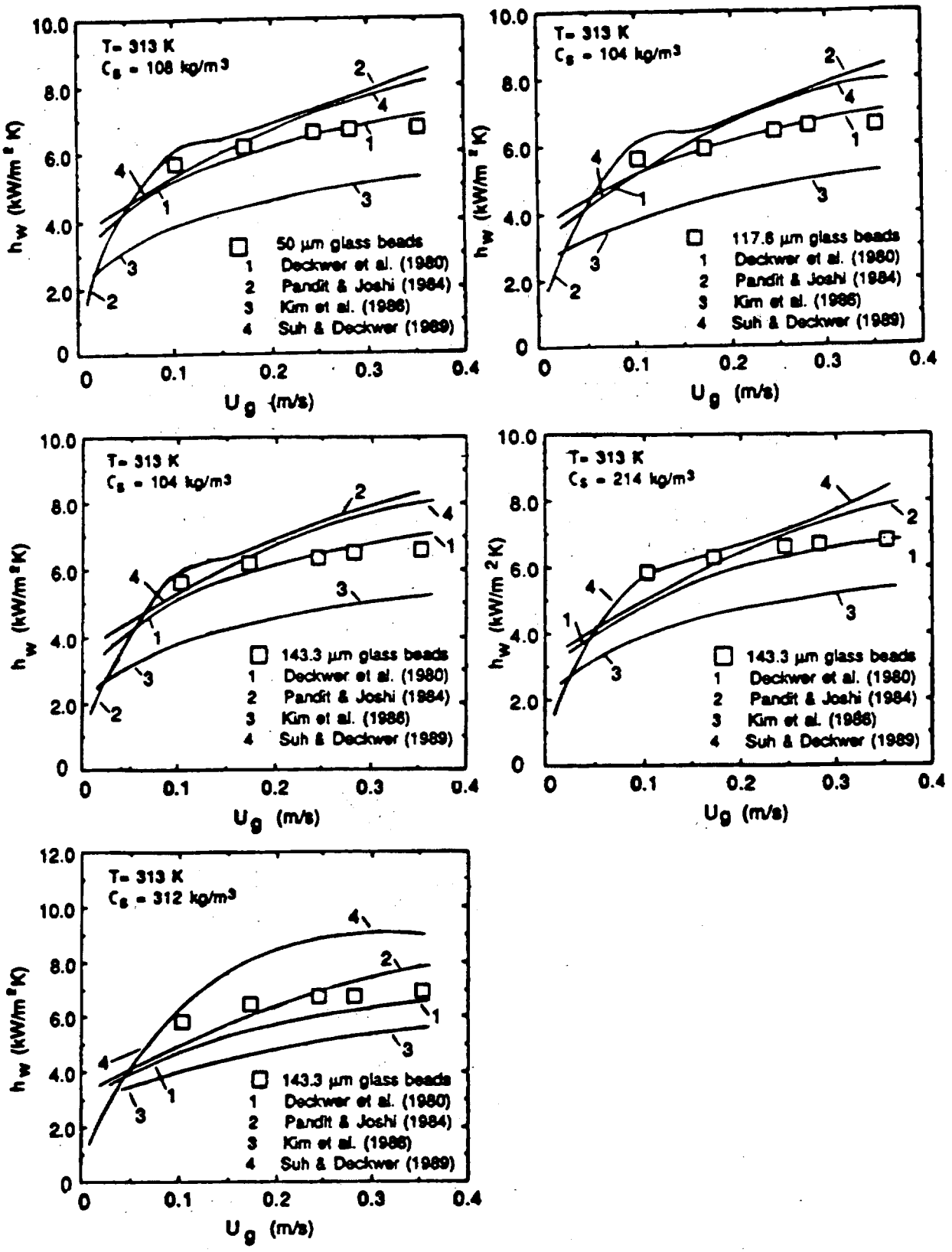

Fig. 6.18. Comparison of h_W data for air-water-glass bead system with different models.

Joshi [106] correlation based values (curve 2) are almost always greater than the experimental values. Deckwer et al. [51], and Suh and Deckwer [109] correlations lead to values which also fail to reproduce the experimental data except the former [51] does slightly better than the latter [109]. However, the agreement between the experimental data and the predictions based on Deckwer et al. [51] correlation consistently worsens as the solids concentration in the slurry increases. In view of the failure of existing correlations, Saxena et al [125] synthesized these data on the basis of Eqs. (6.51) and (6.54) with the constants a, b, c and d listed in Table 6.2. This approach as shown in the concentration and particle dependence of these data on the four constants is rather insignificant and therefore a global fit was tried with the results reported in Table 6.3. The accuracy with which these constants can reproduce the data is also outlined in the last two columns.

Additional data taken for this system for a single probe and a seven-tube bundle [80] were also analysed in a similar fashion with the results reported in Table 6.4. The global constants yielded the following relations:

$$h_w = 8.723\ U_g^{0.194} \qquad 6.57$$

and

$$h_w = 8.108 + 1.508\ \ln U_g \qquad 6.58$$

Here, h_w is in kW/m^2K and U_g in m/s. Comparison of the 130 experimental data points with the corresponding computed values from Eqs. (6.57) and (6.58) is presented in Figs. 6.20 and 6.21 respectively. The agreement is certainly satisfactory in view of the simplicity of relations and neglect of powder size and slurry concentration.

Saxena and Patel [126] have reported data for three single probes of different diameters and correlated the same on the basis of Eq. (6.58). They have proposed a correlation of their data involving a dimensionless hydraulic diameter and air velocity. The final form is:

$$h_W = 9.5\ [1 - (D_T/D_C)]^{0.25}\ U_g^{0.20} \qquad 6.59$$

Table 6.2. Values of the constants of Eqs. (6.51) and (6.54) as determined from the experiemntal h_W values for three different systems in the temperature range 308 - 316K and measured in 0.108 m bubble column equipped with 19 mm heat transfer probe.

System	d_p (μm)	C_s (kg/m^3)	Air Velocity Range (m/s)	Equation (1) a	Equation (1) b	Equation (2) c	Equation (2) d	% Abs. Dev. in h_W Avg.	% Abs. Dev. in h_W Range
Air - Water	-	-	0.103 - 0.353	6.92	0.099	-	-	1.04	0.7 - 2.6
	-	-	0.103 - 0.353	-	-	6.84	0.578	1.03	0.1 - 2.5
Air - Water Magnetite	43.6	107	0.108 - 0.362	7.48	0.109	-	-	1.34	0.2 - 3.0
		167	0.108 - 0.362	8.21	0.164	-	-	1.50	0.1 - 3.4
		258	0.108 - 0.362	7.94	0.131	-	-	1.84	0.3 - 4.9
	43.6	107	0.108 - 0.362	-	-	7.39	0.691	1.32	0.2 - 3.0
		167	0.108 - 0.362	-	-	8.00	1.042	1.52	0.2 - 3.6
		258	0.108 - 0.362	-	-	7.79	0.837	1.78	0.4 - 4.9
Air - Water - Glass Bead	50.0	108	0.103 - 0.353	7.97	0.145	-	-	1.11	0.4 - 1.9
		108	0.103 - 0.353	-	-	7.77	0.901	0.97	0.2 - 1.7
	117.6	104	0.103 - 0.353	7.77	0.142	-	-	1.35	0.4 - 1.8
		104	0.103 - 0.353	-	-	7.59	0.867	1.34	0.5 - 2.1
	143.3	104	0.103 - 0.353	7.61	0.126	-	-	0.92	0.2 - 1.6
		214	0.103 - 0.353	7.81	0.126	-	-	0.60	0.5 - 2.7
		312	0.103 - 0.353	8.07	0.137	-	-	1.01	0.3 - 1.5
	143.3	104	0.103 - 0.353	-	-	7.46	0.769	0.85	0.3 - 1.4
		214	0.103 - 0.353	-	-	7.66	0.791	0.50	0.4 - 2.6
		312	0.103 - 0.353	-	-	7.89	0.875	0.89	0.3 - 1.3

Table 6.3. Global constants of Eqs. (6.51) and (6.52) as determined from the experimental h_W values for air-water-magnetite and air-water-glass bead systems in the temperature range 308 - 316K and measured in 0.108 m bubble column equipped with 19 mm heat transfer probe.

System	a	b	c	d	% Abs. Dev. in h_W	
					Avg.	Range
Air - Water -	7.89	0.136	-	-	1.8	0.02 - 6.2
Magnetite	-	-	7.74	0.865	1.8	0.01 - 6.1
Air - Water -	7.84	0.135	-	-	1.7	0.10 - 4.0
Glass Bead	-	-	7.68	0.841	1.7	0.01 - 4.2

Table 6.4. Values of the constants of Eqs. (6.51) and (6.54) as determined from the experimental h_W values for air-water and air-water-glass bead systems at 393K and measured in 0.108 m bubble column equipped with a 19 mm single tube and a seven-tube bundle.

	d_p (μm)	w_s (%)	a	b	% Abs. Dev.		c	d	% Abs. Dev.	
					Avg.	Range			Avg.	Range
SINGLE TUBE	-	0	8.224	0.193	4.188	1.44-6.85	7.55	0.958	3.224	1.68-6.01
	50	10	7.645	0.170	0.902	0.09-2.28	7.269	0.890	1.297	0.03-2.85
	119	10	8.611	0.181	0.990	0.04-2.40	8.156	1.052	1.373	0.10-2.94
	143	10	8.516	0.172	1.433	0.03-3.07	8.08	0.994	1.046	0.02-2.16
SEVEN-TUBE BUNDLE	-	0	8.645	0.197	3.101	1.12-6.84	8.00	1.050	1.780	0.02-4.53
	50	5	8.706	0.190	2.067	0.33-5.68	8.07	1.021	1.135	0.19-4.48
	50	10	9.207	0.203	2.793	0.41-5.87	8.446	1.113	1.335	0.10-4.51
	119	5	8.980	0.205	2.335	0.31-5.12	8.291	1.127	1.400	0.22-3.79
	119	10	8.953	0.194	2.027	0.17-4.59	8.360	1.105	2.082	0.11-3.78
	143	5	8.732	0.195	2.060	0.16-4.94	8.099	1.052	1.214	0.18-3.85
	143	10	8.619	0.193	2.137	0.54-4.54	8.036	1.044	1.175	0.03-2.97
	143	20	9.263	0.208	2.618	0.07-5.58	8.444	1.135	1.818	0.31-3.92
	143	30	9.189	0.209	2.334	0.01-5.37	8.401	1.144	1.827	0.57-4.28

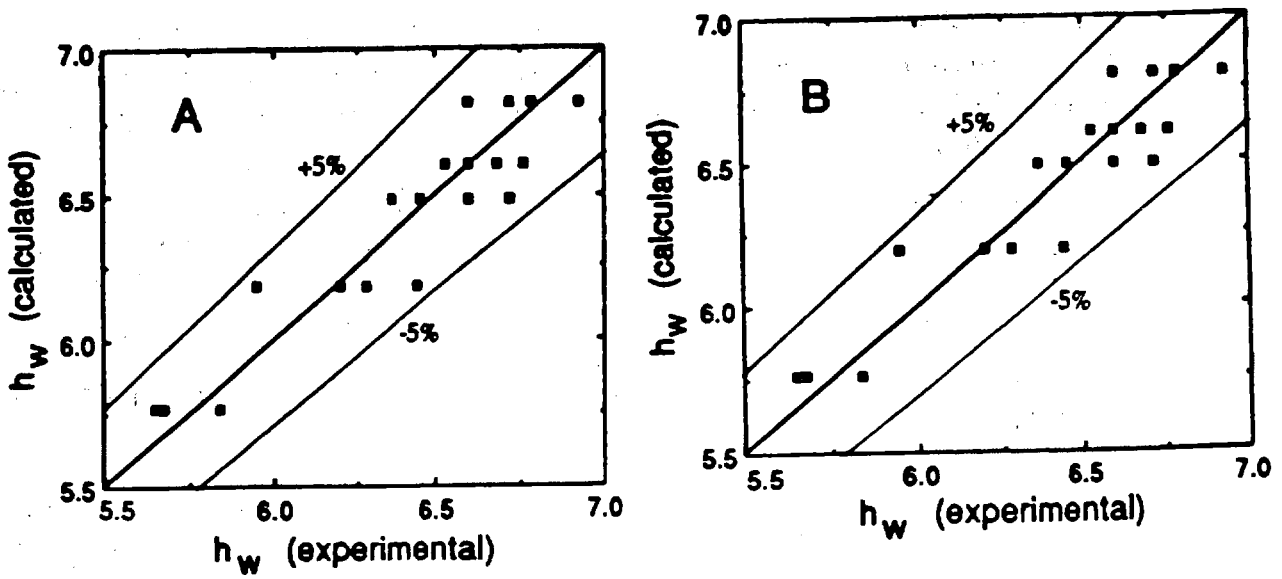

FIG 8.

Fig. 6.19. Parity plot of h_W (kW/m^{2}K) for air-water-glass bead system: (A) power function, and (B) logarithmic function.

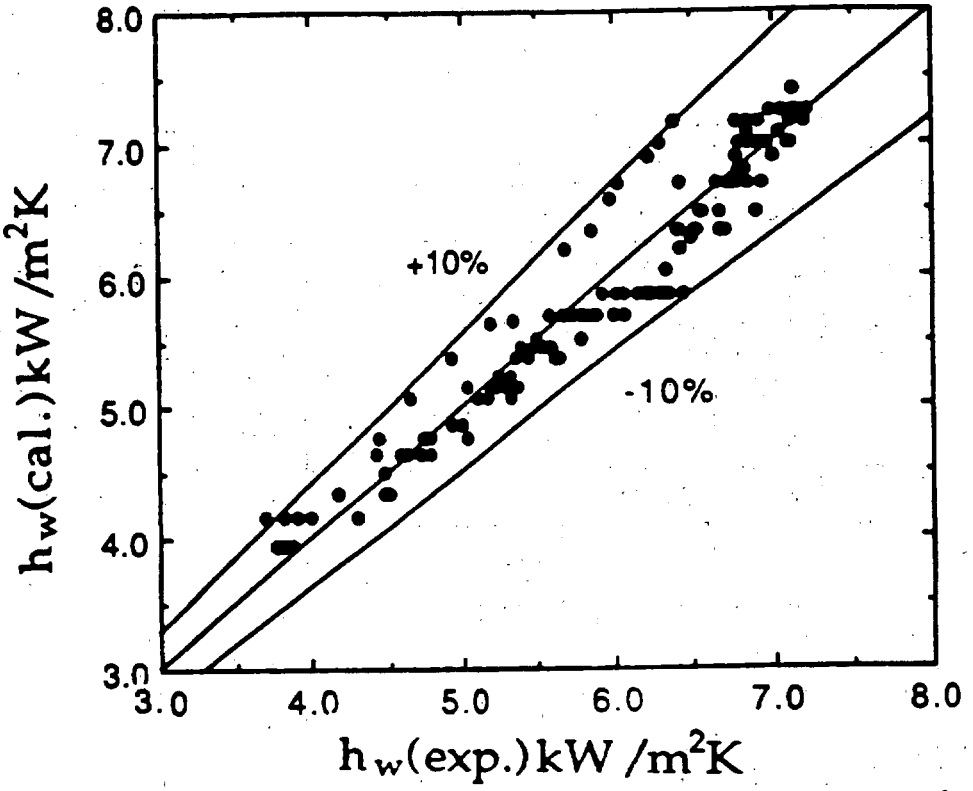

Fig. 6.20. Comparison of experimental and calculated heat transfer coefficient values with global constants for power function, Eq. (6.57).

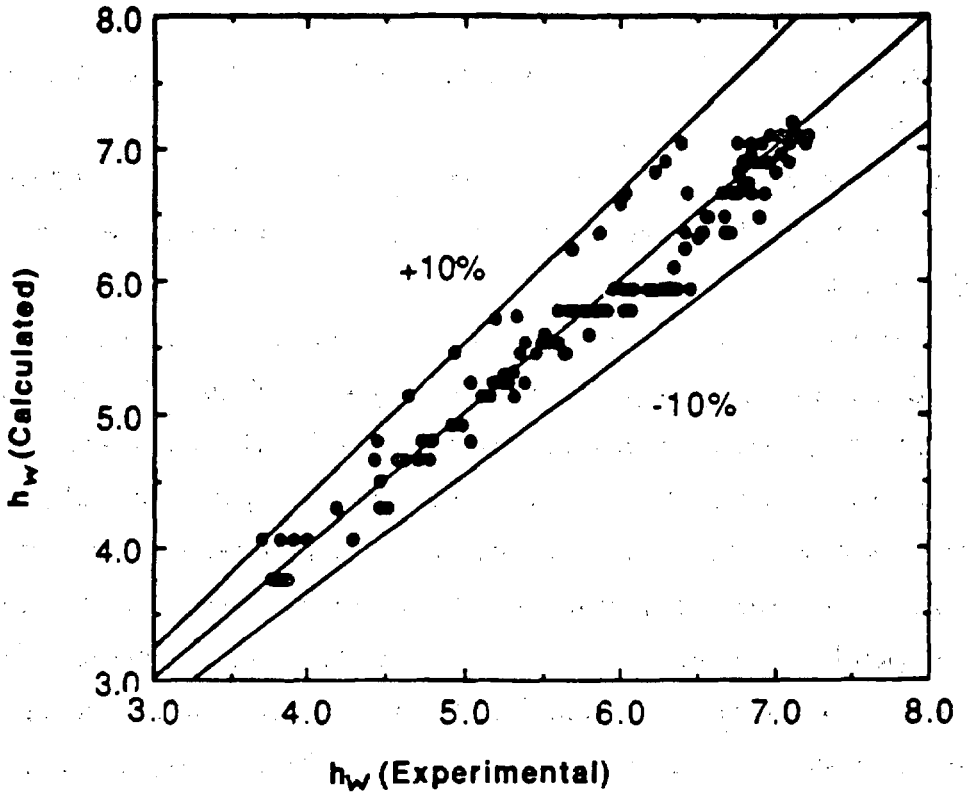

Fig. 6.21. Comparison of experimental and calculated heat transfer coefficient values with global constants for semi-logarithmic function, Eq. (6.58).

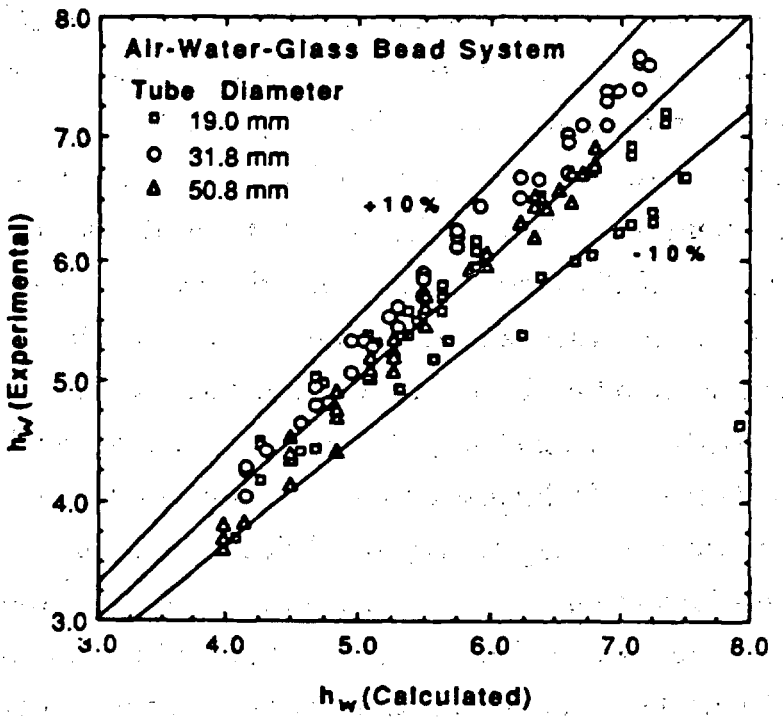

Fig. 6.22. Comparison of experimental and calculated values of heat transfer coefficient on the basis of the proposed correlation.

Comparison of data with the corresponding predictions based on Eq. (6.59) is presented in Fig. 6.22.

In the larger column air-water-glass bead system has been investigated [111, 112] with seven- and thirty-seven tube bundles, and the same are presented in Figs. 4.69 through 4.74.

The heat transfer coefficient values for the seven-tube bundle averaged over the slurry concentration and particle size range, as shown in Fig. 6.23, are compared with the predictions of four models. The Pandit and Joshi correlation [106] has the same deficiency for this three-phase system at all the three temperatures as discussed earlier for the two-phase (air-water) in connection with Fig. 6.5. The correlation underpredicts the data and has an improper qualitative dependence on air velocity. The Deckwer et al. correlation [51] leads to values which are increasingly smaller than the experimental values as the temperature increases. However, the shape of qualitative dependence of heat transfer coefficient on air velocity is well reproduced. The Kim et al. model [107] leads to values which are still smaller than the predicted values based on the Deckwer et al. correlation [51]. Attempts of Suh and Deckwer [109] to improve the correlation of Kim et al. [107] seem to be only partially successful. This correlation does reproduce the qualitative shape of the dependence of heat transfer coefficient on air velocity, and quantitatively leads to values which are in the best agreement with the experimental data of all the four correlations. However, the degree of disagreement between theory and experiment is large and the predictions are systematically smaller than the observed values. It would be appropriate to refine this model as more data become available.

Kolbel et al. [100] and Kato et al. [110] have proposed correlations which also include the particle size. We discuss these correlations for slurry bubble columns because our measurements suggest very small dependence on particle diameter. Both these correlations predict much higher values than the experimental data. The Mersmann et al. correlation [103] as generalized by Saxena et al. [105] for the three-phase systems leads to the maximum heat transfer coefficient values which are smaller than the experimental values. The disagreement, which is about 35 percent at 303 K, increases to about 60 percent at 343 K. In summary, the available heat transfer models and correlations are inadequate to predict the

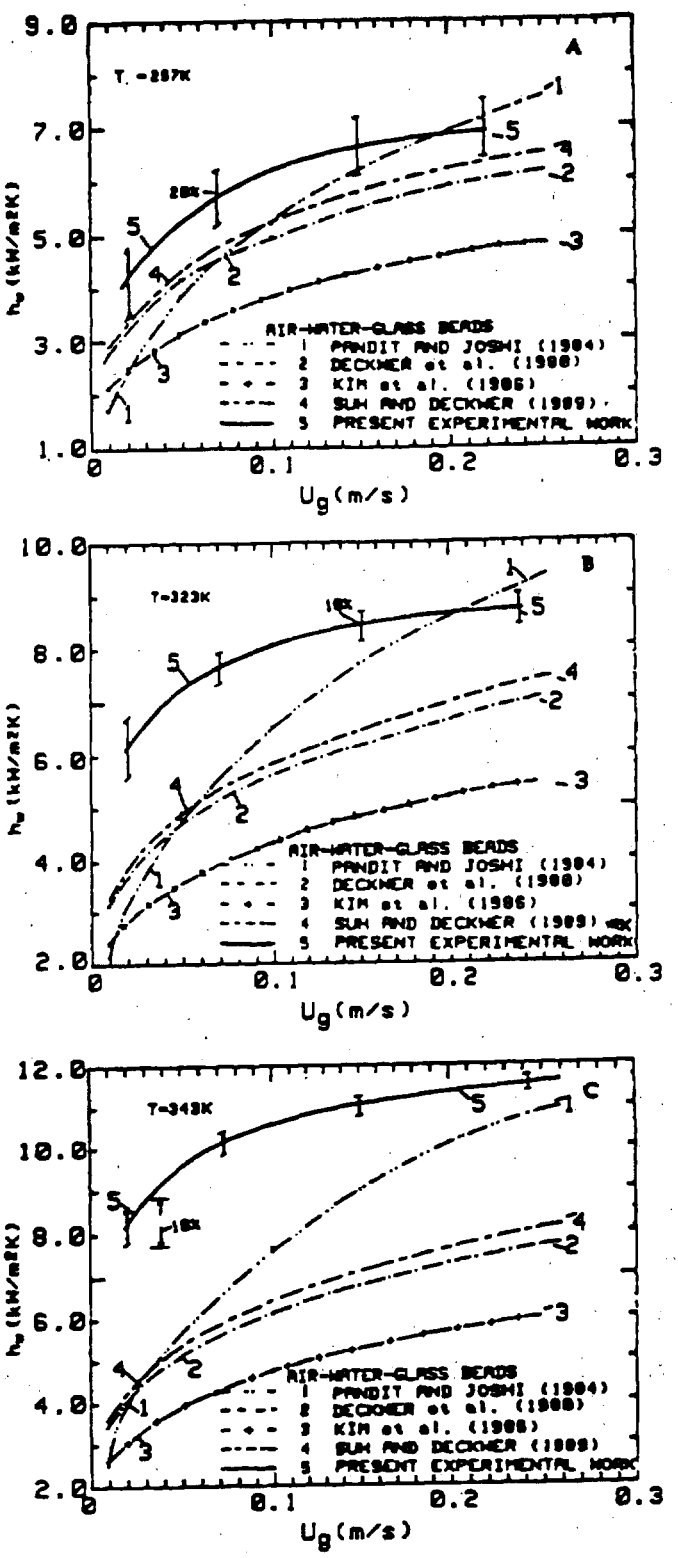

Fig. 6.23. Comparison of averaged heat transfer coefficient values as a function of air velocity with the predictions of different correlations at (A) 297, (B) 323, and (C) 343K.

experimental data, particularly as the temperature increases above the ambient.

The heat transfer data obtained for the thirty-seven tube bundle are compared with the four model predictions in Fig. 6.24. In all cases, the theoretical values are consistently and appreciable smaller than the experimental values. The models either predict very small or no dependence on slurry concentration. In view of the failure of models, a semitheoretical correlation is presented in Fig. 6.8. The computed values are in good agreement with the experimental values in all cases and it is recommended as a good empirical correlation.

The comparison of h_w values [105, 128] for the air-water-magnetite system for a single probe in the small column, Fig. 4.34, are compared with the predictions of five models in Fig. 6.25.

Computed values of h_w from Deckwer et al. correlation [51] are shown in Fig 6.25 (curves 1) as a function of air velocity and for two extreme compositions of the solids in the slurry. The computed values exhibit a continuous increase in the values of h_w with increase in U_g. For values of U_g greater than 0.1 m/s, the experimental values are almost constant, and therefore the agreement between the experimental and calculates values worsens with increase in air velocity. The experimental data show almost no dependence on solids concentration in the slurry while the calculated values exhibit an increase in the value of h_w with increase in solids concentration over the entire range of air velocities. The theory is a reasonable representation of experimental data at air velocities smaller than 0.1 m/s.

Computed values of heat transfer coefficient from the correlation of Pandit and Joshi [106] are shown in Fig. 6.25 (curves 2) as a function of air velocity. h_w values increase with U_g for all particle sizes in disagreement with the experimental data which exhibit an almost constant value for all velocities greater than 0.1 m/s. The computed data also show a dependence on solids concentration, h_w values are greater for slurries containing a larger weight fraction of solids. This difference in h_w values is also dependent upon the size of solids and increases appreciably for slurries containing particles of average diameter of 90.5 μm and greater. The reproduction of h_w by this model is inferior to that of Deckwer et al. model [51] over the entire air velocity range.

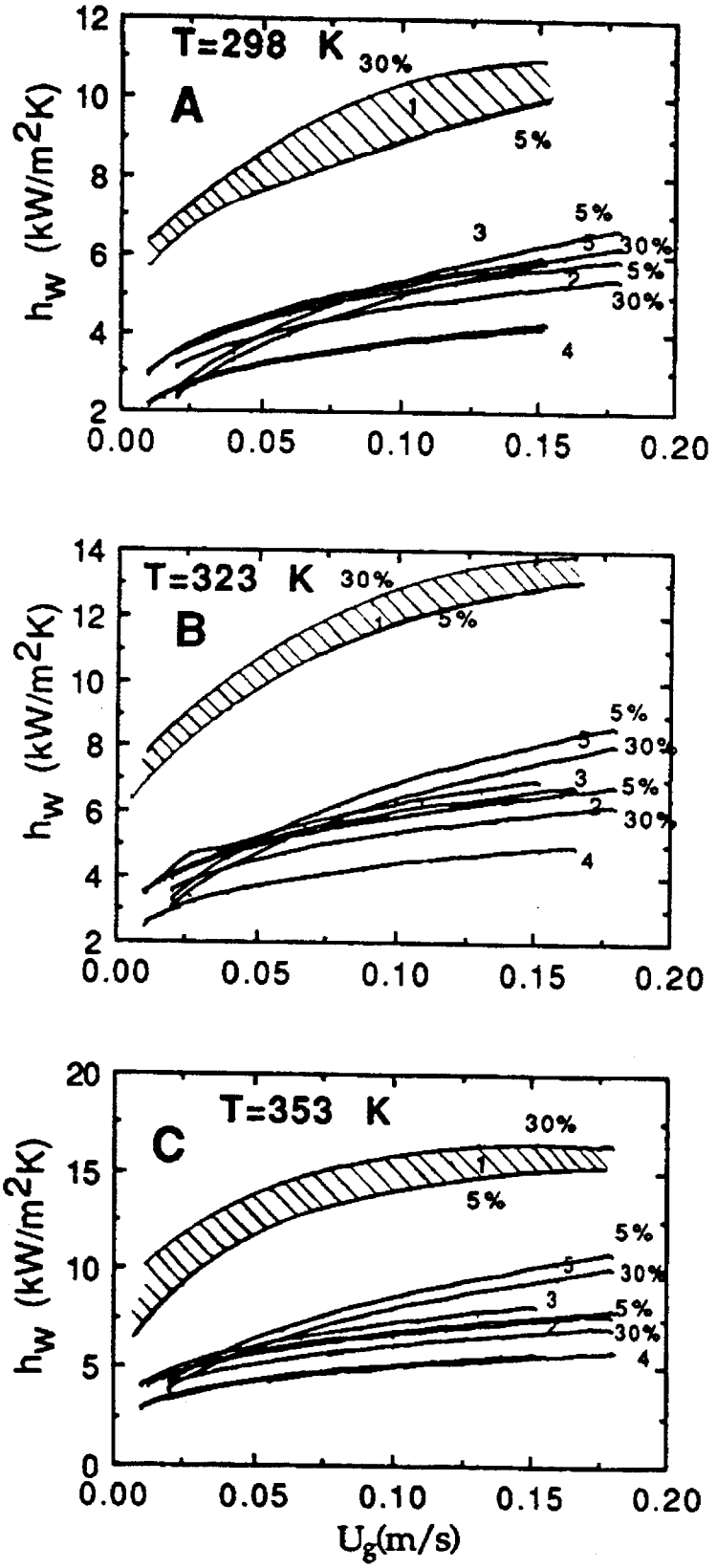

Fig. 6.24. Comparison of experimental heat transfer coefficients with the predictions of different models for the air-water-glass bead system, (1-Experimental, 2-Deckwer, 3-Suh and Deckwer, 4-Kim et al., 5-Pandit and Joshi).

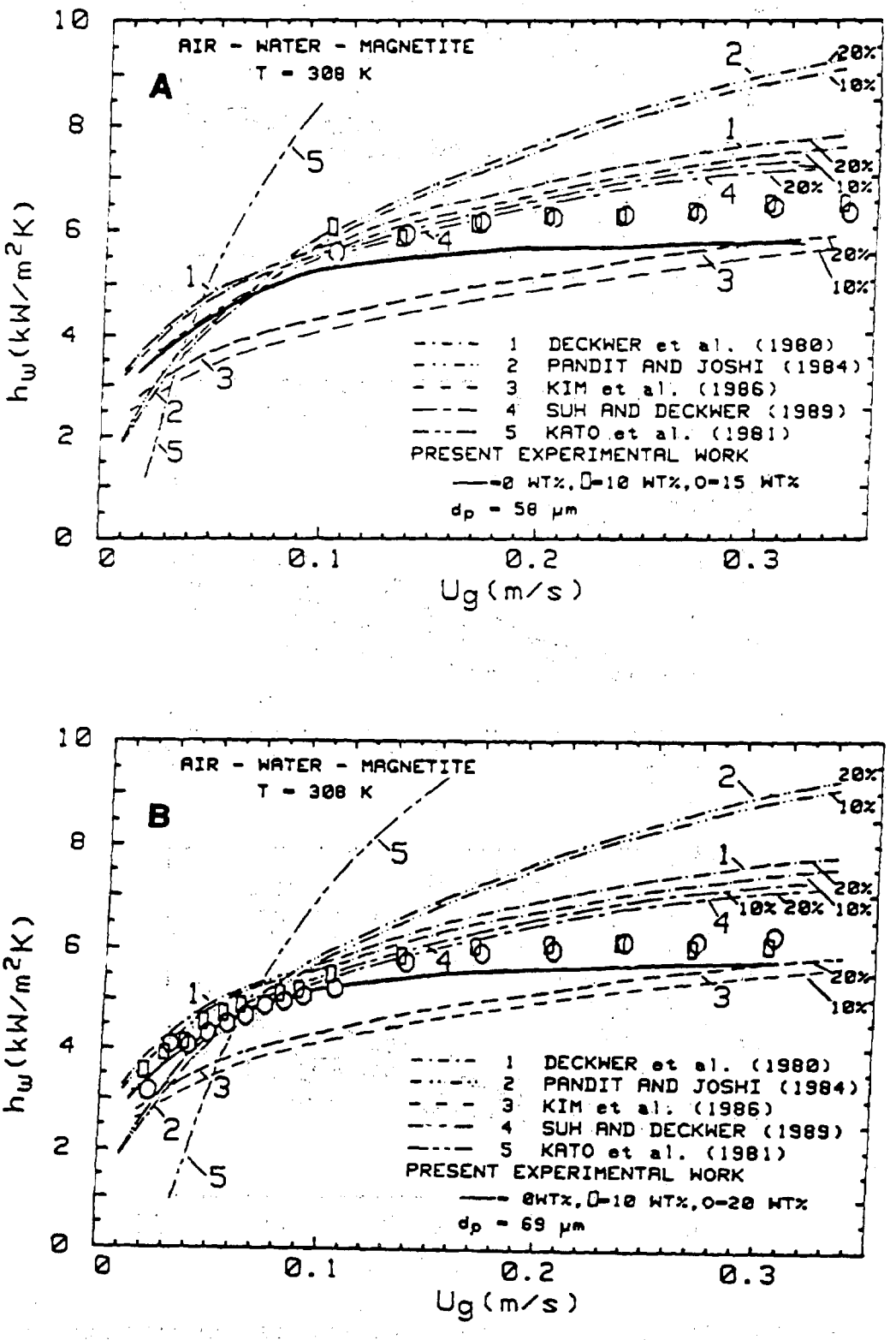

Fig. 6.25. Comparison of heat transfer data with the predictions of different models.

The qualitative shape of h_w dependence on U_g for air velocities smaller than 0.1 m/s is different as predicted on this model than found in present experiments.

Computed values of h_w from Kim et al. correlation [107] as a function of air velocity are shown in Fig. 6.25 (curves 3), and these are in unsatisfactory agreement with the experimental values. The correlation based values exhibit a dependence on solids concentration in the slurry, the values exhibit a dependence on solids concentration, the increase is more for particles of average diameter 90.5 μm and greater. These trends are not exhibited by the experimental data. The calculated values are invariably smaller than the experimental values over the entire air velocity range. This correlation which is primarily developed for liquid fluidized beds appear to be inadequate for slurry bubble columns.

Computed values from Suh and Deckwer [109] of h_w (curves 4) are in somewhat better agreement with experimental data at lower air velocities (smaller than 0.1 m/s) than from Kim et al. correlation [107]. At higher air velocities, the computed values are greater than the experimental values, while those based on Kim et al. [107] are smaller than the experimental values. Other trends for the two sets of values are indeed identical.

It can be seen apriori that Eq. (6.48) will not be very appropriate for reproducing the experimental data in view of its pronounced dependence on d_p while experimentally determined h_w values are almost independent of d_p. In Fig. 6.25 are graphed the computed h_w values from Eq. (6.48) for different experimental conditions as a function of air velocity. In each case the calculated values are poor representation of the experimental data. The calculated h_w values increase much faster with air velocity and fail completely to reproduce the experimental data. The relatively better reproduction of the experimental values as the particle size increases is a consequence of the procedure adopted in developing the correlation. In general, this correlation is regarded as inadequate for representing the experimental heat transfer data for slurry bubble columns.

Computed values of $h_{w\,max}$ from the relations of Eq. (6.25) for 10, 10 and 30 weight percent of solids in the slurry are 4.50, 4.64 and 5.03 kW/m^2K. The corresponding experimental values range between 6.0 to 6.4 kW/m^2K. This agreement of theory and experimental is regarded as fair and reasonable but not

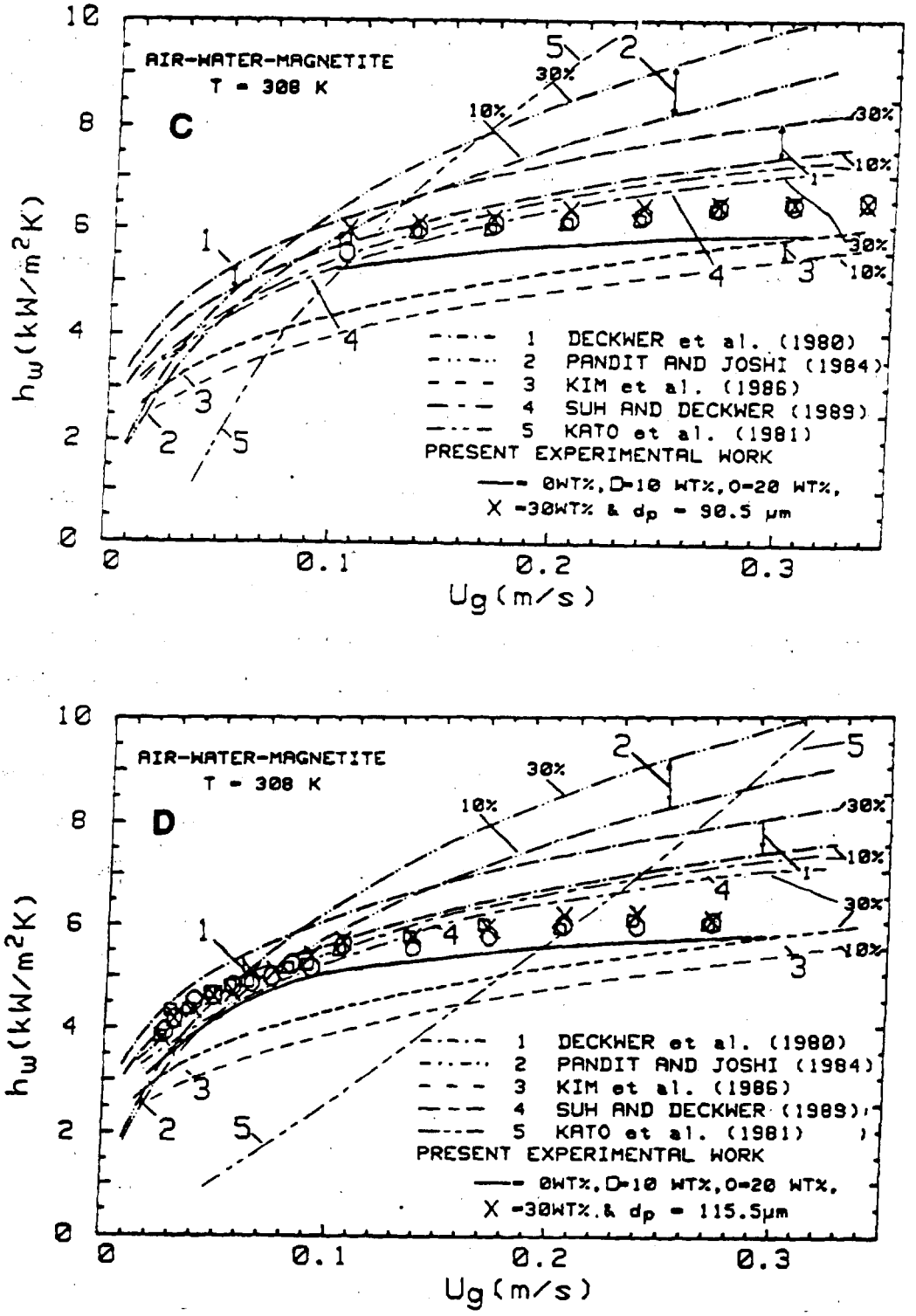

Fig. 6.25. Comparison of heat transfer data with the predictions of different models.

satisfactory.

In view of the failure of these models to represent h_W data, the empirical Eqs. (6.51) and (6.54) were employed to correlate the data with the results reported in Table 6.5 and in Figs. 6.26 and 6.27. The agreement of theory and experiment is quite good, the deviations between the two sets of values are always within the estimated uncertainty of 5%. The maximum percentage average absolute deviations for the 102 data points are 1.4 and 1.3 respectively for the power and semi-logarithmic functions. The corresponding percentage maximum deviations are 4.3 and 4.1 respectively. Experimental h_w data are considered up to a maximum gas velocity of 0.15 m/s where h_w invariably gets to a constant value.

Since the constants of Eqs. (6.51) and (6.54) so not differ significantly with the change of particle size and concentration in the slurry, a global fit based on the entire data was tried with the following results:

$$h_w = 9.206\, U_g^{0.233} \qquad 6.60$$

and

$$h_w = 7.805 + 1.056 \ln U_g \qquad 6.61$$

Based on these two relations, comparison of experimental and calculated h_w values is presented in Figs. 6.28 and 6.29. The functions of Eqs. (6.60) and (6.61) are adequate to estimate h_w data within an average absolute and maximum deviations of 2.9 and 2.7, and 15 and 12 percent respectively. This is quite remarkable as the small dependencies of h_w on d_p and w_s are ignored in this correlation.

From Table 6.5, this exponent has an average value of 0.244 for slurries containing particles of 69 μm average diameter and smaller, while its value is 0.20 for slurries having average diameter of 115.5 μm and larger. This would suggest that for at least larger particles the assumed energy dissipation by viscous forces due to micro-scale eddies in the radial direction which are locally isotropic is not completely valid. Further, as pointed out by Deckwer and coworkers the

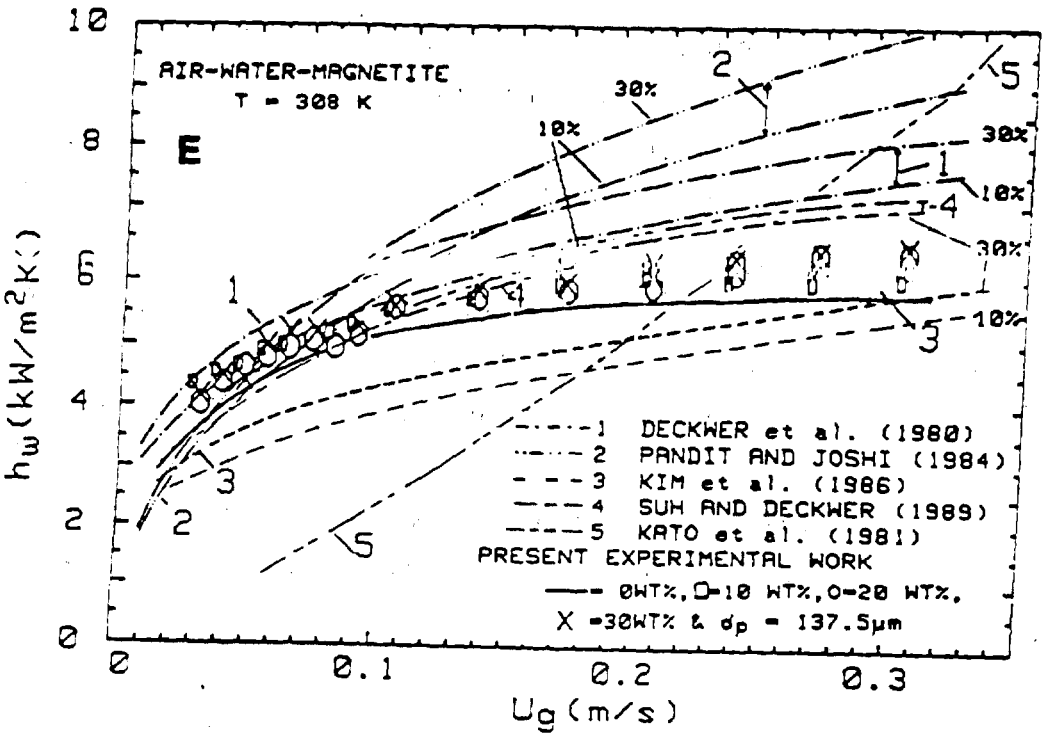

Fig. 6.25. Comparison of heat transfer data with the predictions of different models.

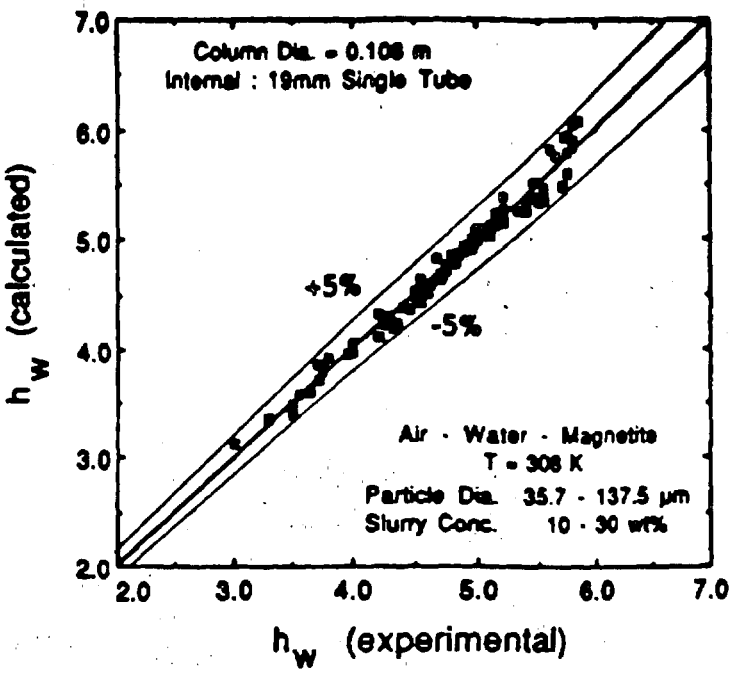

Fig. 6.26. Parity plot for heat transfer coefficient (kW/m^2K). Calculated values are based on Eq. (6.51).

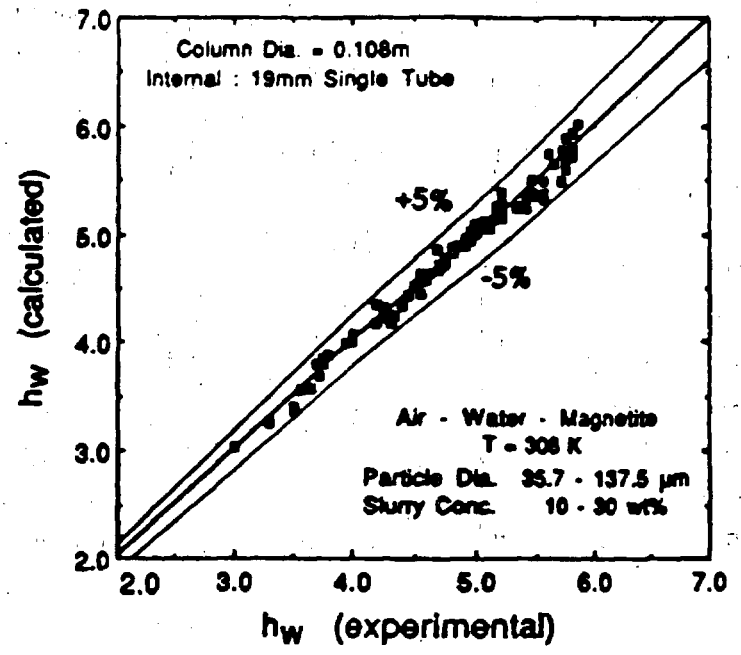

Fig. 6.27. Parity plot for heat transfer coefficient (kW/m^2K). Calculated values are based on Eq. (6.54).

Table 6.5. Values of the constants of Eqs. (6.51) and (6.54) as determined from the experimental h_W values for air-water-magnetite system at 308K and measured in 0.108m bubble column equipped with a 19 mm single heat transfer probe.

d_p	w_s			% Abs. Dev.				% Abs. Dev.	
(μm)	(%)	a	b	Avg.	Range	c	d	Avg.	Range
35.7	10	9.92	0.274	1.67	0.16-4.3	7.93	1.164	1.08	0.22-3.7
49.0	10	9.07	0.236	1.06	0-3.3	7.64	1.039	1.15	0.03-4.1
69.0	10	8.69	0.218	1.12	0.13-2.2	7.49	0.974	1.34	0.03-4.1
69.0	20	9.50	0.249	1.45	0.34-3.6	7.86	1.096	1.13	0.05-3.8
115.5	10	8.47	0.201	1.72	0.19-4.2	7.49	0.940	1.65	0.67-3.1
115.5	20	8.44	0.196	1.62	0.03-3.9	7.49	0.925	1.48	0.35-2.5
115.5	30	9.21	0.223	1.55	0.05-4.1	7.94	1.059	1.39	0.40-3.7
137.5	10	8.40	0.193	0.75	0.27-1.6	7.60	0.959	0.64	0.11-1.8
137.5	20	8.69	0.200	1.63	0.09-3.9	7.80	1.008	1.76	0.18-3.8
137.5	30	8.92	0.203	1.74	0.19-3.8	7.98	1.036	1.75	0.27-2.8

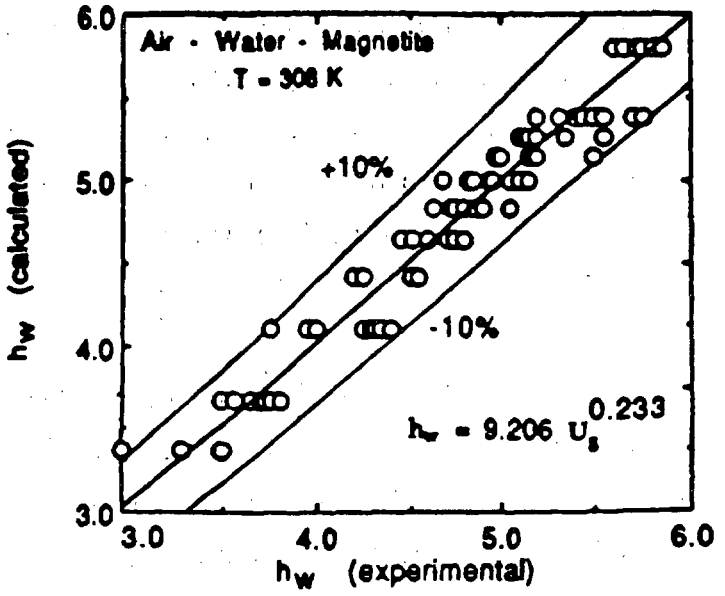

Fig. 6.28. Comparison of experimental and calculated heat transfer coefficient (kW/m^2K) based on Eq. (6.60).

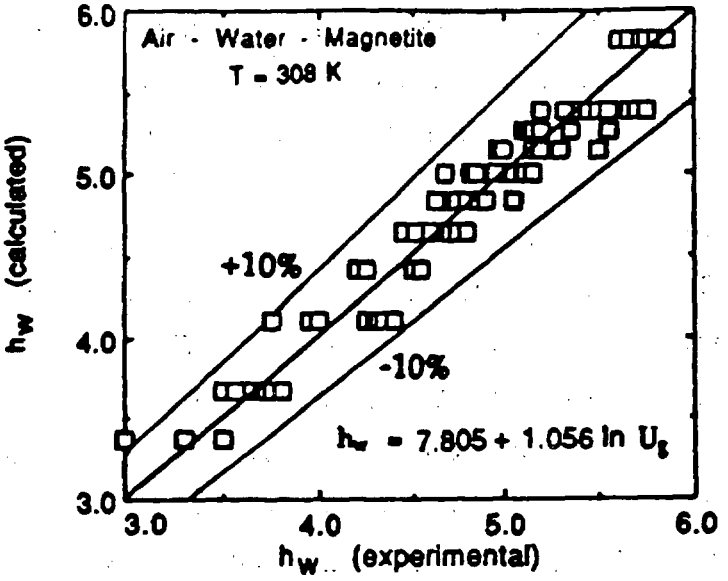

Fig. 6.29. Comparison of experimental and calculated heat transfer coefficient (kW/m^2K) based on Eq. (6.61).

heat transfer for large particles can be augmented by the direct participation of solid particles which will enhance the exchange frequency of fluid elements at the heat transfer surface. On the other hand for small particles the suspension is more homogenous and the variations in h_w will be caused more by the changing thermophysical properties and the experimental work, with micron-size particles, seem to indicate that viscosity of the slurry plays an important role and an empirical multiplicative term is essential.

The air-water-magnetite data [122] for 43.6 μm particles are shown compared with the predictions of various models. It is clear from Fig. 6.30 that the models are inadequate. The empirical Eqs. (6.51) and (6.54) could reproduce the data satisfactorily as seen from Table 6.2. The global constants given in Table 6.3 could reproduce the data as shown in Fig. 6.31.

Experimental data taken for this system in the larger column with a seven-tube bundle are compared with the predictions of various correlations in Figs. 6.32 and 6.33. The experimental data are almost considerably greater than the model based values and both the qualitative and quantitative agreement between theory and experiment is totally unsatisfactory. The empirical relation of Eq. (6.51) on the other hand accomplishes this satisfactorily as shown in Fig. 6.33, which also includes air-water system. The values of the two constants are listed in Table. 6.6.

The experimental data taken in the small column for nitrogen-Therminol-magnetite for a 19 mm single probe [114] are shown compared with the predictions of four models in Fig. 6.34. Deckwer et al. [51] model predicts the data reasonably well. Suh and Deckwer [109] reproduce the two-phase data but fail to reproduce the slurry concentration dependence. Kim et al. [107], and Pandit and Joshi [106] fail to reproduce the experimental data completely in as much as the predictions are too low and the concentration dependence is much less than what is observed experimentally. In Fig. 6.35, the experimental data are compared with the predictions of an empirical Eq. (6.51), where a and b are listed in Table 6.7 for each slurry concentration and three single probes. The reproduction is considered satisfactory.

Next an attempt was made to correlate all the data for the three-probes by a single correlation involving properties of the system and dimensions of the

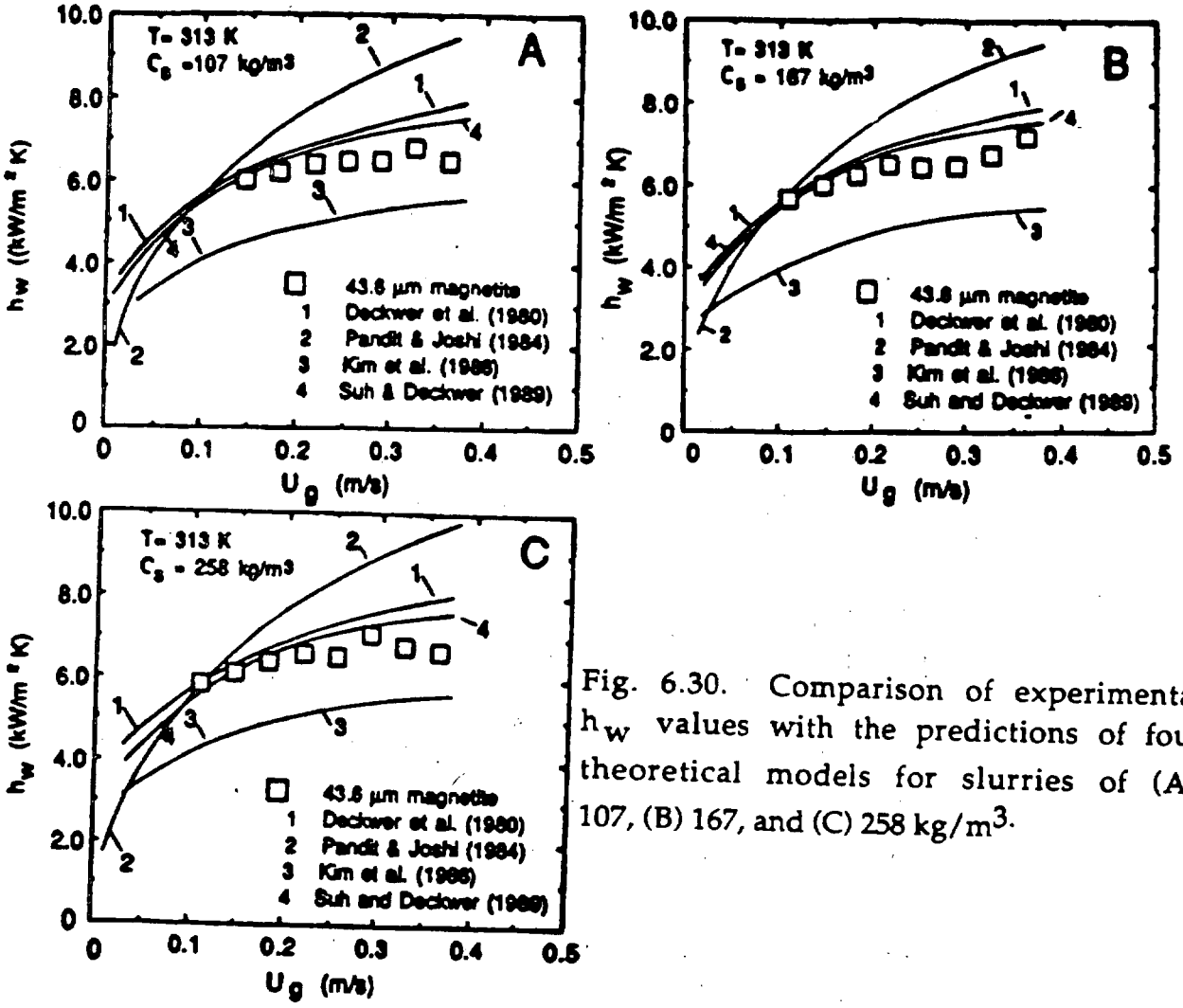

Fig. 6.30. Comparison of experimental h_w values with the predictions of four theoretical models for slurries of (A) 107, (B) 167, and (C) 258 kg/m^3.

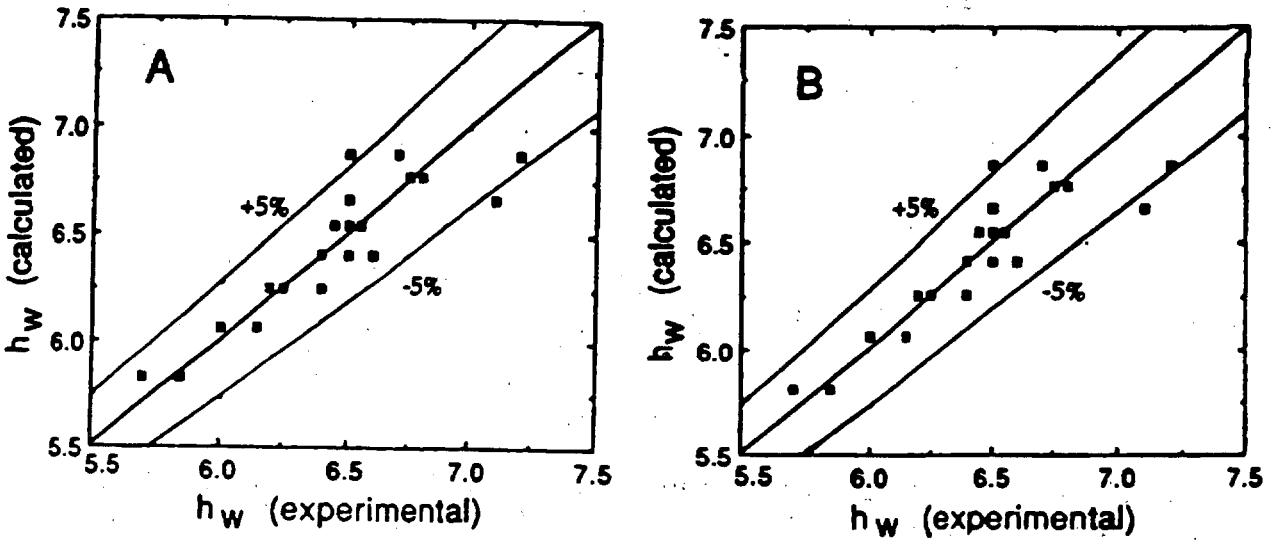

Fig. 6.31. Parity plot of h_W (kW/m^{2}K) for air-water-magnetite system: (A) power function, and (B) logarithmic function.

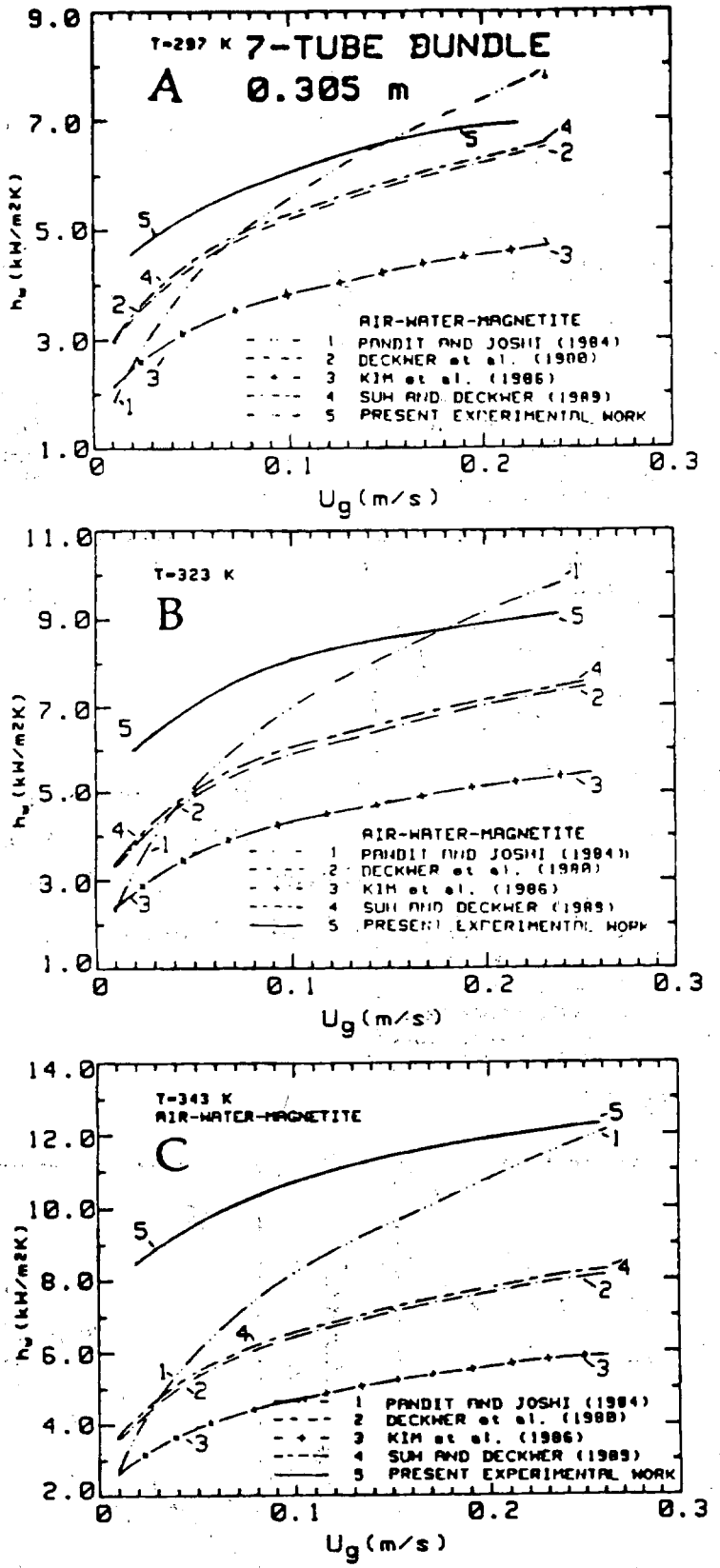

Fig. 6.32. Comparison of averaged experimental heat transfer coefficient with the predictions of different correlations at (A) 297, (B) 323, and (C) 343K.

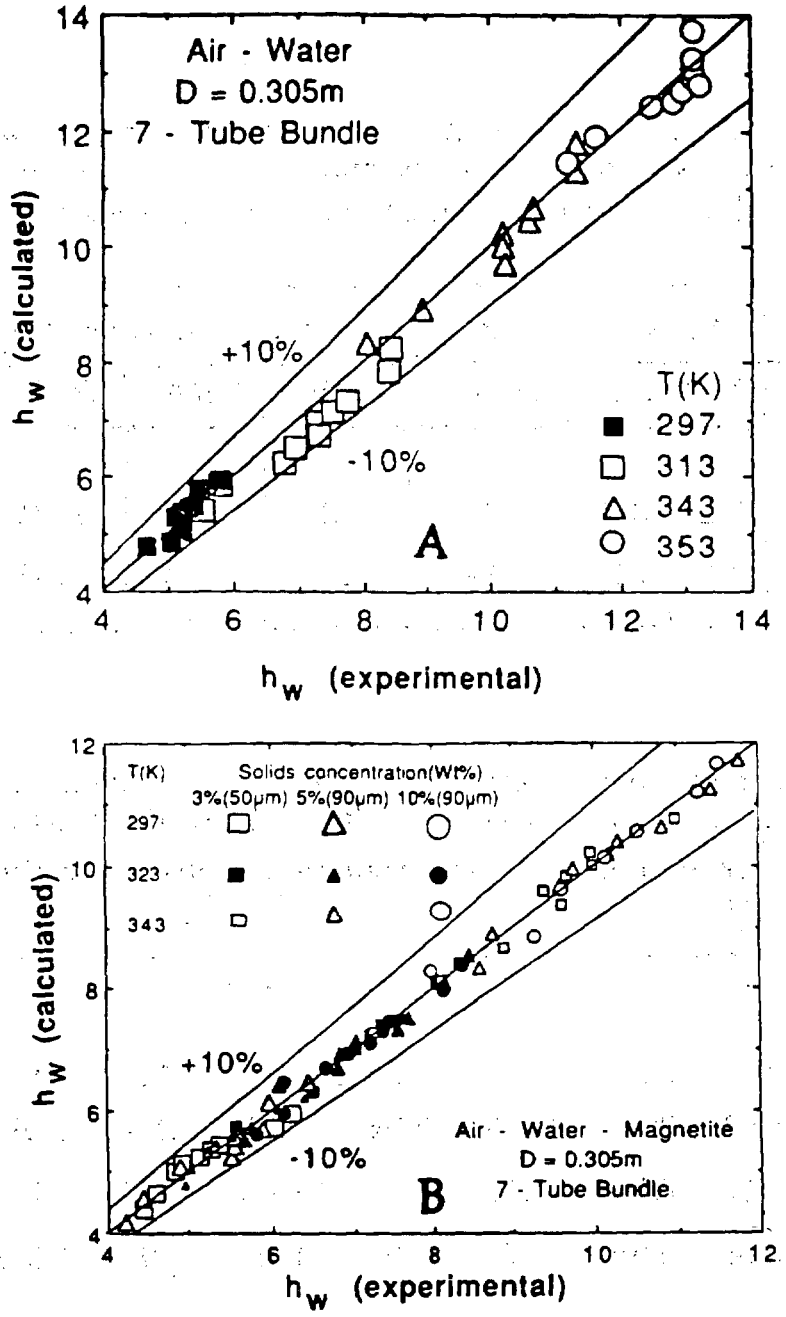

Fig. 6.33. Correlation of heat transfer data on Eq. (6.51) for (A) air-water, and (B) air-water-magnetite systems.

Table 6.6. Values or the constants of Eq. (6.51) as determined from the experimental h_W values for air-water and air-water-magnetite systems and measured in 0.305 m bubble column equipped with a seven-tube bundle.

Constant	Air-Water System			Air-Water-magnetite System		
	297K	313K	343K	297K	323K	343K
a	7.32	12.27	15.87	8.77	11.42	15.41
b	0.11	0.20	0.16	0.16	0.16	0.15

Table 6.7. Values of the constants of Eq. (6.51) as determined from the experimental h_W values for nitrogen-Therminol-magnetite system at 306 - 312K and measured in 0.108 m bubble column equipped with three single heat transfer probes.

Probe Diameter	$w_S = 0$		$w_S = 15$		$w_S = 30$		$w_S = 50$	
mm	a	b	a	b	a	b	a	b
19.0	0.913	0.283	0.969	0.266	1.037	0.261	1.265	0.276
31.8	0.810	0.238	0.856	0.287	0.933	0.295	1.284	0.340
50.8	0.656	0.268	0.800	0.295	0.745	0.242	1.016	0.340

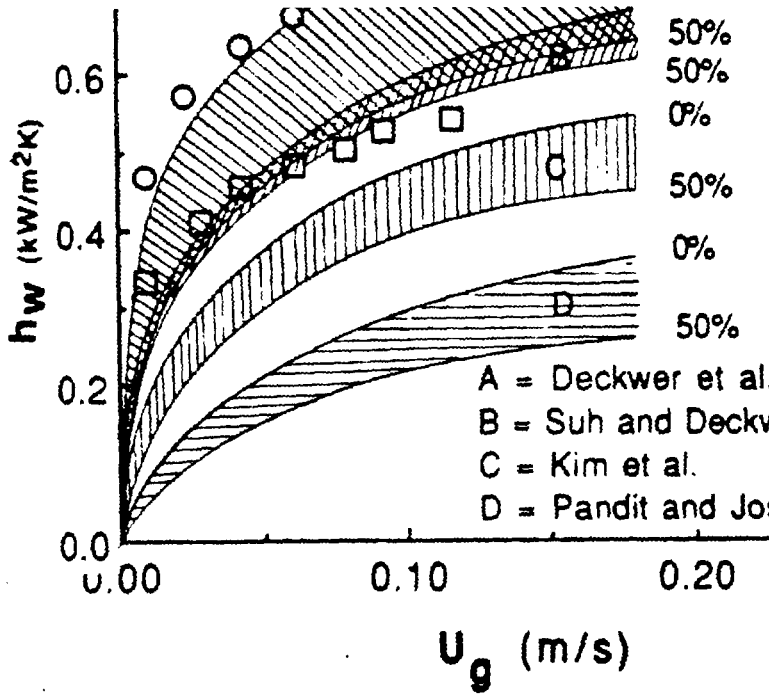

Fig. 6.34. Comparison of experimental data (o-0%, O-50%) for 1
with the theoretical predictions. A: Deckwer et al. [51], B: Suh
[109], C: Kim et al. [107], and D: Pandit and Joshi [106].

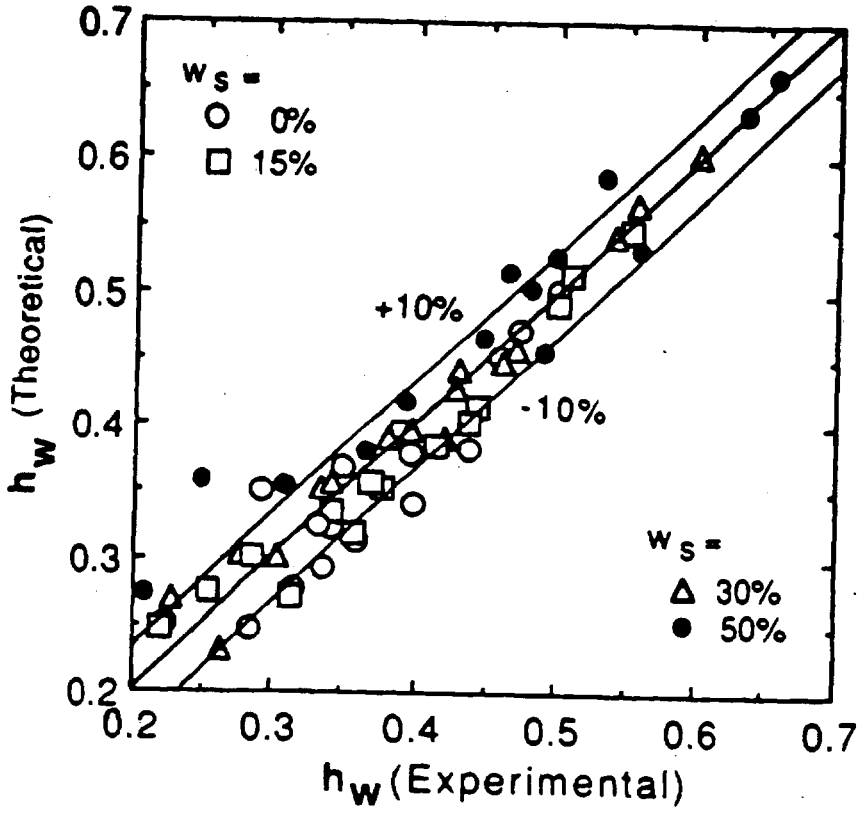

Fig. 6.35. Comparison of experimental and computed h_W values according to Eq. (6.51).

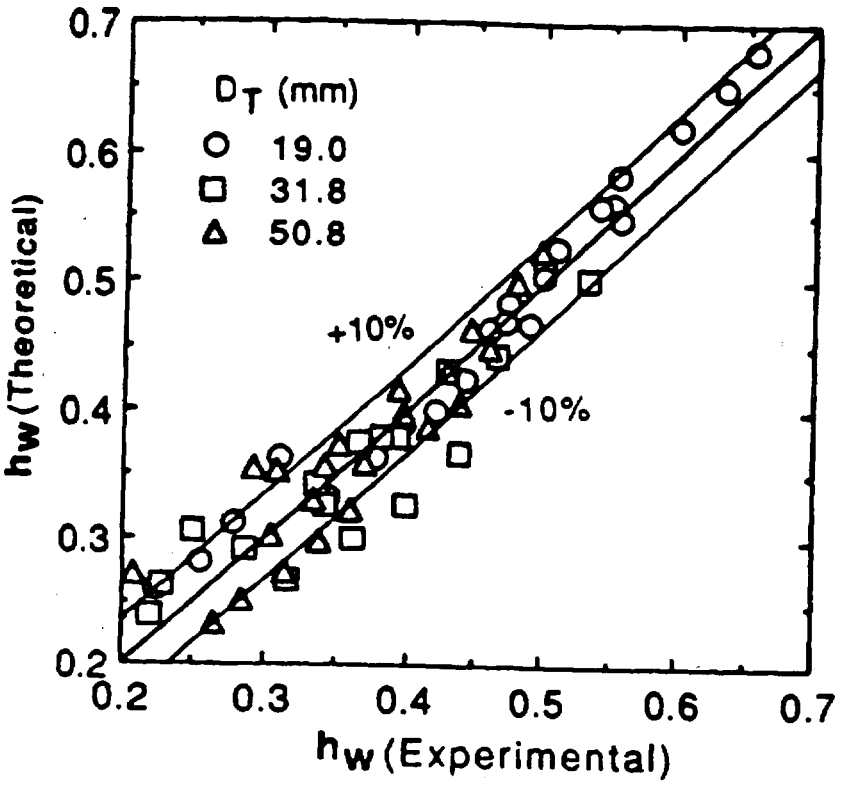

Fig. 6.36. Comparison of experimental and computed h_W values according to Eq. (6.62).

baffled bubble column. Calculations revealed that such properties as thermal conductivity, density and heat capacity change in such a fashion that their product is approximately constant. Hence viscosity essentially plays a dominant role. Further, on the basis of Table 6.7 a mean value of 0.27 was taken for the exponent of U_g. This yielded a correlation of the following form:

$$h_w = 1.05 \, (\mu_L/\mu_{SL})^{-0.6} \, (U_g)^{0.27} \, [\, (D_c - D_T) / D_c \,]^{0.65} \qquad 6.62$$

Explicit comparison of experimental data points with the predictions of Eq. (6.62) is shown in Fig. 6.36 and it is regarded as quite satisfactory.

The experimental data for the seven-tube bundle and magnetite powders of average diameters 27.6 and 36.6 μm [115] are shown compared with the model predictions in Fig. 6.37. Again, the models fail to predict the experimental data. The form of Eq. (6.51) on the other hand could synthesize the data as shown in Fig. 6.38. It is seen that the exponent of U_g varies appreciably and the coefficient of U_g even more. The latter is because of the changes in the rheology of the system and Deckwer's theory [51, 93] does not simulate these changes in slurry properties with composition.

The experimental data for the nitrogen-Therminol-magnetite (d_p = 36 μm) system taken in the larger column with thirty-seven tube bundle [121] are shown plotted in Fig. 6.39 as a function of U_g in log-log plot. Each data set referring to a particular temperature can be represented by an empirical relation of the type of Eq. (6.51). The values of the two constants are listed at each temperature in Fig. 6.39. b is strongly temperature dependent and much different from 0.25. It increases with temperature in the foaming region (T>423 K) and decreases with temperature in the nonfoaming region (T<423 K).

The experimental data [114] for the air-water-silica sand system are reported in Fig. 4.68 for a seven-tube bundle in the larger column at three different temperatures and two slurry concentrations. In Fig. 6.40, the data are shown compared with the predictions of four models. The nature of disagreement between the calculated and experimental h_w values is dependent on temperature and it gets poorer as the temperature increases.

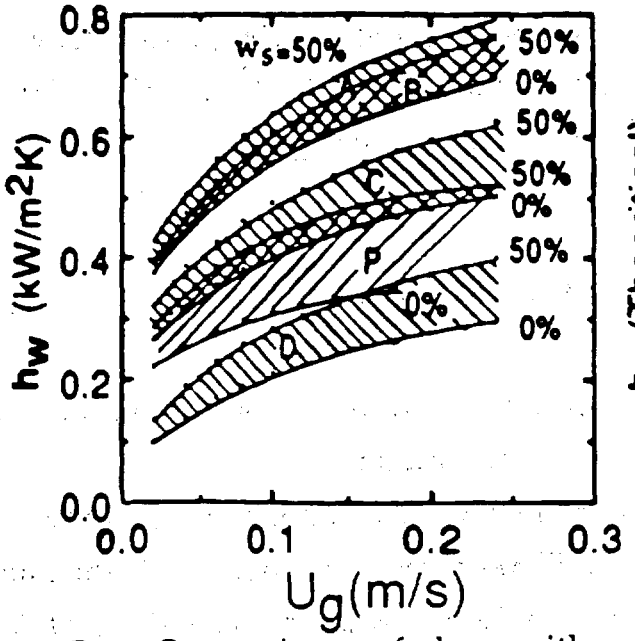

Fig. 6.37. Comparison of h_w with model predictions. A-[51], B-[109], C-[107], D-[106] and P- Present work.

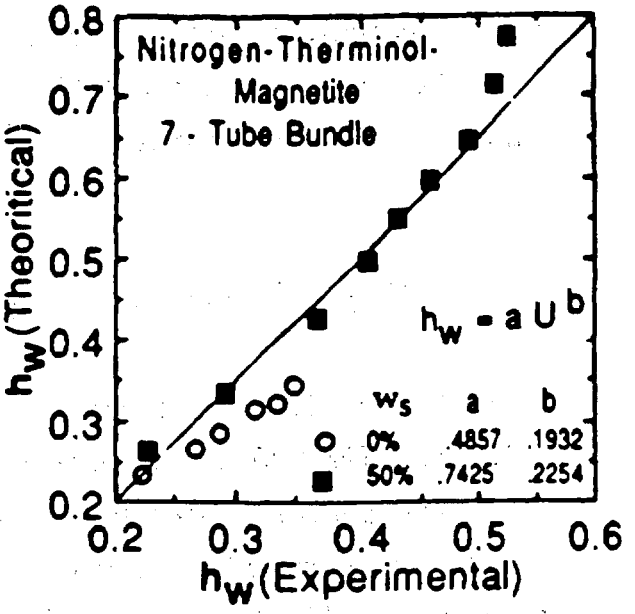

Fig. 6.38. Comparison of experimental h_w values with a semi-theoretical correlation(Eq.6.51).
(6.60). (6.61).

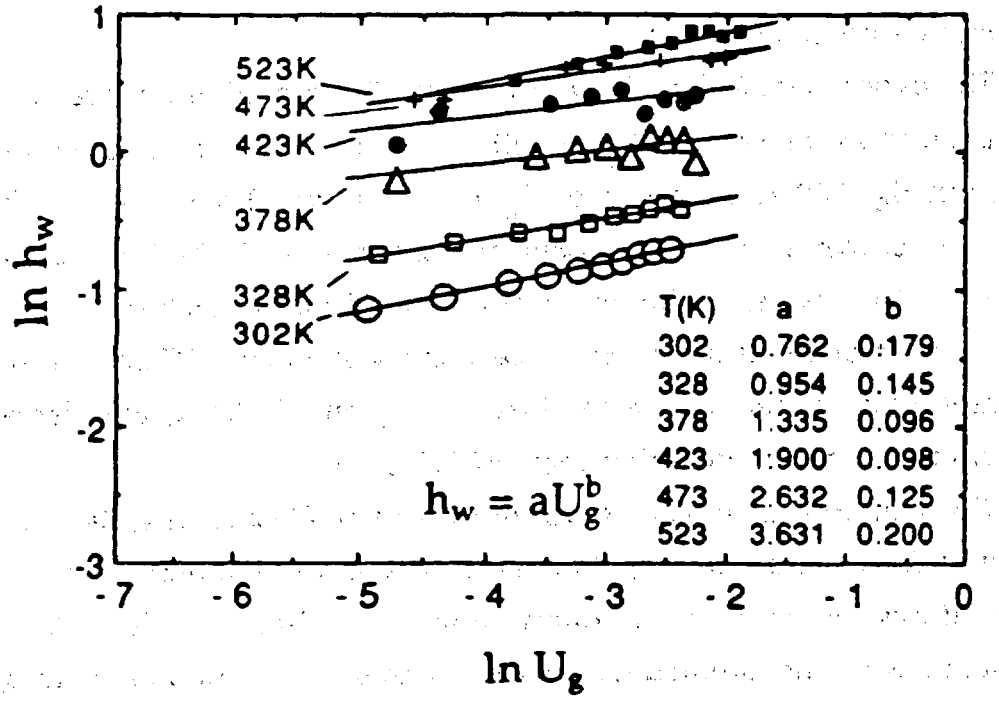

Fig. 6.39. A plot of heat transfer coefficients(probe 1) versus nitrogen velocity shown in logarithmic coordinates at different temperatures. Solids concentration = 40 wt%.

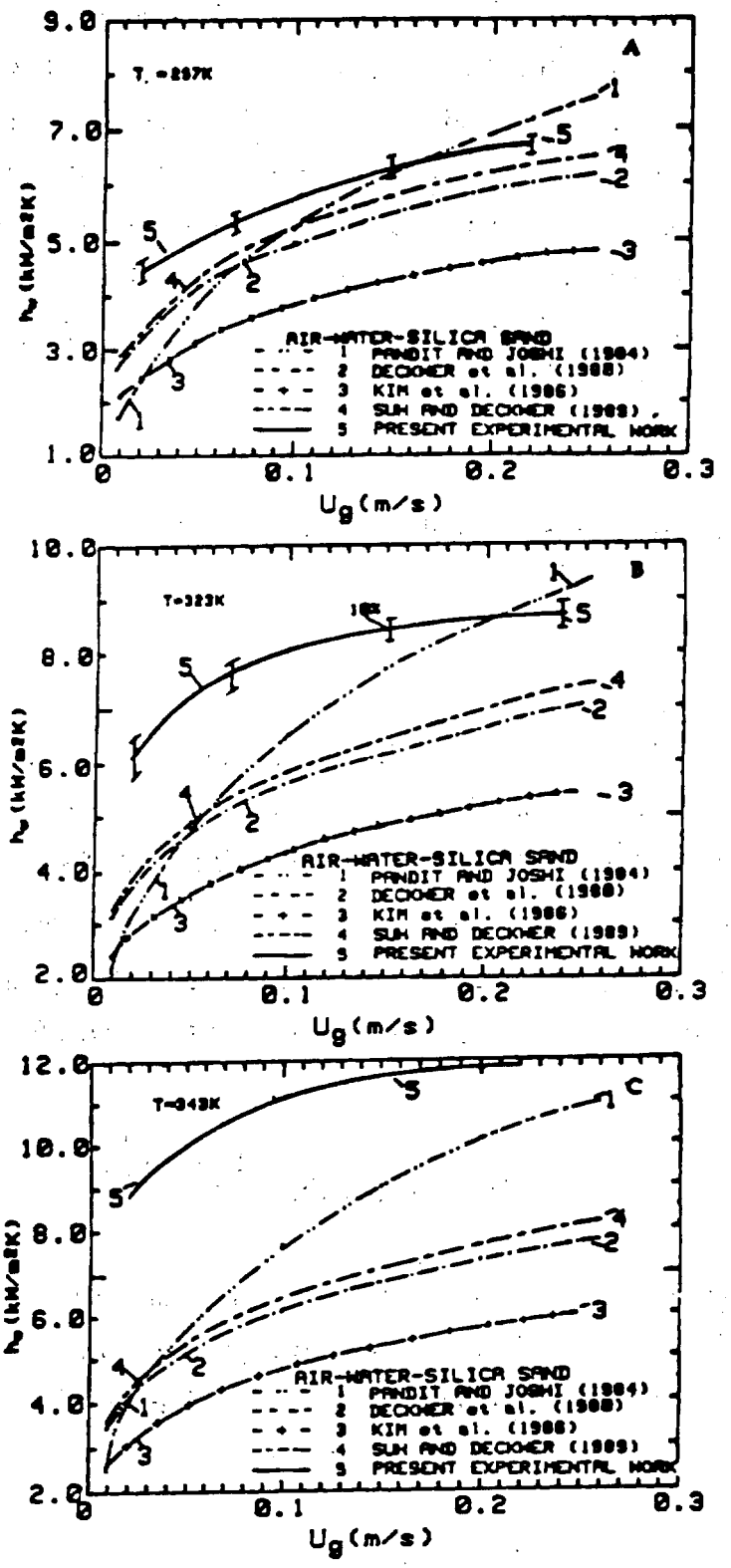

Fig. 6.40. Comparison of the concentration averaged heat transfer coefficient values as a function of air velocity with the predictions of different correlations at temperatures of 297(A), 323(B) and 343K(C).

A semi-empirical approach based on Eq. (6.51) has been tried mainly to understand the nature of dependence of b on the system properties. The values of a and b obtained by regression analysis are given in Table 6.8. It is to be noted that the values of b varies over a range and are significantly different from 0.25. It may also be emphasized that the values of a are dependent on temperature and slurry composition for the system. Comparison of experimental and computed values is shown in Fig. 6.41. According to Deckwer [93], and Deckwer et al. [51] h_w is given by:

$$h_w(kW/m^2K) = 0.0001(k\rho C_p)_{SL}^{0.5} (\rho g/\mu)_{SL}^{0.25} U_g^{0.25} \qquad 6.63$$

$$\equiv a' U_g^{0.25} \qquad 6.64$$

Attempts to correlate the h_w data at each temperature on the basis of Eq. (6.64) yielded results reported in Table 6.8. It is clear that a choice of 0.25 for b is inappropriate as it fails to reproduce the experimental data. Calculations revealed that for the present systems $(k\rho C_p)_{SL}$ varies only within $\pm$ 2 percent. The major changes in h_w creep in through changes $(\rho g/\mu)_{SL}$. Matching experimental data with Eq. (6.63) suggests the following relation for h_w:

$$h_w(kW/m^2K) = 3.5 \times 10^{-6} (k\rho C_p)_{SL}^{0.5} (\rho g/\mu)_{SL}^{0.47} U_g^{0.25} \qquad 6.65$$

Equation (6.65) reproduces the data with an average absolute deviation of 13 percent, the range being 3 - 26. The corresponding numbers for Eq. (6.63) are 29 and 6 - 55 respectively. In summary, the existing theory of Eq. (6.63) is not substantiated by present data both for a or a', and b.

6.5. Conclusions and Recommendations

Our extensive results of heat transfer coefficient measurement from simulated heat transfer surfaces of tubes of different diameters and tube bundles

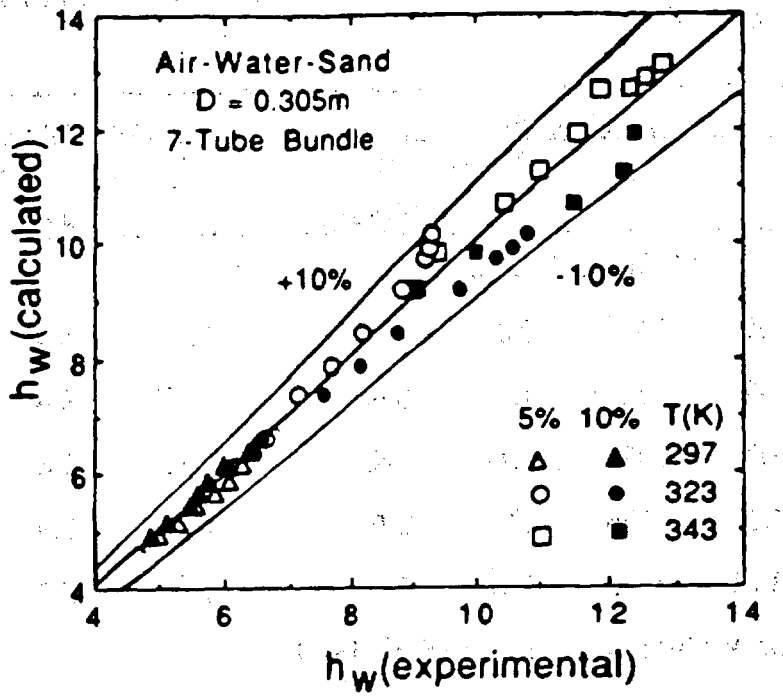

Fig. 6.41. Comparison of experimental and calculated (Eq. 6.51) h_W (kW/m^2K) values for the air-water-silica sand system.

Table 6.8. Values of the constants of Eqs. (6.51) and (6.64) as determined from the experimental h_W values for air-water and air-water-sand systems at several temperatures and measured in 0.305 m bubble column equipped with a seven-tube bundle.

T (K)	Equation (5)				Equation (7)		
	a	b	% Abs. Dev.		a'	% Abs. Dev.	
			Avg.	Range		Avg.	Range
	Air-Water System						
303	7.59	0.119	2.0	0.1-9	11.3	8.4	3-16
313	8.99	0.125	4.1	3-8	12.5	9.8	2-14
323	11.23	0.178	6.1	1-9	14.8	9.6	2-16
333	12.68	0.166	5.7	2-9	17.1	7.9	2-17
343	13.01	0.177	5.1	3-8	19.6	5.8	2-18
	Air-Water-Sand System (5-10 Wt%)						
297	7.85	0.125	2.5	0.8-3	11.4	8.9	1-15
323	13.38	0.199	4.1	2-8	15.6	5.6	2-12
343	17.21	0.160	4.7	1-7	23.7	8.7	2-30

of different configurations and sizes in two bubble columns as a function of gas velocity at different temperatures and involving dispersions of two different liquids (water and Therminol) and solids of different physical properties, sizes and size ranges, have lead to results which may be synthesized in terms of several general conclusions. The scope of this section is to briefly enumerate them and also include the information generated regarding the ability of model expressions and correlations to predict heat transfer coefffcient for design and scaleup purposes. This summary is to precipitate certain concrete recommendations for future research in the area of heat transfer in slurry bubble columns

For all two-phase and three-phase systems, the heat transfer coefficient is found to increase monotonically with air velocity, first rapidly and then slowly and finally approaches to a constant value in the fully developed churn-turbulent flow regime. The heat transfer coefficient is temperature dependent and in general increases with increase in temperature . Similarly, the influence of liquid phase viscosity is pronounced on heat transfer coefficient and it is found to decrease appreciably as the viscosity increases. The difference in h_w for systems involving water and Therminol-66 is more than an order of magnitude. It would be interesting to investigate several liquids of distinctly different viscosity values and at several temperatures. Such data are essential because of the unknown and involved relationship between the viscosity of a liquid and temperature . A good knowledge of the understanding of the viscosity of a liquid on different parameters characterizing its structure and temperature is essential.

The dependence of heat transfer coefficient on the nature of solids present in the three-phase systems is interesting. For fine micron-size range iron oxide powders, it is found that the presence of solids increases the heat transfer coefficient, and increased concentration of solids in the slurry augments the heat transfer coefficient relatively more than in dilute concentrations. It is considered, based on limited data, that the heat transfer rate enhancement occurs through the changes in the rheology of the suspension. For larger particles, the heat transfer coefficient increases but this increase is much more pronounced for slurries involving a liquid of higher viscosity, Therminol-66 versus water. The heat transfer rate augmentation now probably occurs through the direct

participation of the solid phase. Again this is an important feature from a practical stand point. In direct coal liquefaction plants, catalyst particles of a size range are employed and concentrations can be quite high and the temperature of operation is high so that all the three interacting parameters (viscosity, particle size, or size range and slurry viscosity) must be considered to establish the heat transfer rates. At the present time, not enough knowledge exists to resolve these interacting parameters and their influence on heat transfer rates in a unique manner and both theoretical and experimental research is required for the proper understanding.

The influence of internals present in the column on heat transfer rates is also complicated and significant. Experiments have indicated that the presence of tube bundles present in the column increases the heat transfer coefficient by improving the liquid circulation and mixing in the bubble column so that the heat transfer surface is bathed more frequently and more efficiently by the liquid or slurry suspension elements or packets. The same circumstance is created by an increase in the column diameter and hence we have seen an appreciable increase in heat transfer rates of unbaffled columns as the column diameter increases from 0.108 m to 0.305 m. However, the present work also suggests that well baffled bubble columns (columns with tighter tube bundles) will exhibit only feeble dependence of heat transfer coefficient on column diameter. Small diameter bubble columns with single probes can be modelled on the basis of dimensionless hydraulic diameter. The tube-bundle pitch effect could not be established on the basis of present work and to resolve this feature a well planned more elaborate experimental effort will be in order.

The present experimental effort has clearly demonstrated that heat transfer rates increase with increase of solids in the column as long as these can be uniformly suspended, and the presence of heat exchanger surfaces further augments the heat transfer rates by improving the degree of liquid mixing. This is a very useful result and at least qualitative guidance can be drawn from our work for the design of practical slurry bubble column. For quantitative simulation more detailed experimental work will be in order. This is particularly interesting because the available correlations and model-based experssions fail both qualitatively as well as quantitatively to represent the body

of data generated in the present program. We have found an empirical approach to correlate experimental data but to put it on a more fundamental basis further research is needed which is beyond the scope of the present contract.